DESIGN OF AlGaN/GaN BASED HEMT FOR LOW NOISE AND HIGH-SPEED APPLICATIONS

Project report submitted
in partial fulfilment of the requirement for the degree of

Bachelor of Technology

By

CHANDRAV JYOTI MEDHI (200610026016)

SHRESTA DAS (200610026051)

SHREYA SENGUPTA (200610026052)

SUBHRANIL DEY (200610026056)

Under the guidance
of

Mr. NIRANJAN JYOTI BORAH
Assistant Professor
Dept. of Electronics and Telecommunication Engineering

DEPARTMENT OF ELECTRONICS & TELECOMMUNICATION ENGINEERING

ASSAM ENGINEERING COLLEGE

JALUKBARI- 781013, GUWAHATI

June, 2024

ASSAM ENGINEERING COLLEGE, GUWAHATI

CERTIFICATE

This is to certify that the thesis entitled “Design of AlGaN/GaN based HEMT for Low Noise and High-Speed Application” submitted by Chandrav Jyoti Medhi (200610026016), Shresta Das (200610026051), Shreya Sengupta (200610026052) and Subhranil Dey (200610026056) in the partial fulfillment of the requirements for the award of Bachelor of Technology degree in Electronics & Telecommunication Engineering at Assam Engineering College, Jalukbari, Guwahati, is an authentic work carried out by them under my supervision and guidance.

To the best of my knowledge, the matter embodied in the thesis has not been submitted to any other University/Institute for the award of any Degree or Diploma.

Signature of Supervisor

Mr. Niranjan Jyoti Borah

Asst. Professor, Dept. of ETE

Assam Engineering College

June, 2024

DECLARATION

We declare that this written submission represents our ideas in our own words and where others' ideas or words have been included, we have adequately cited and referenced the original sources. We also declare that we have adhered to all principles of academic honesty and integrity and have not misrepresented or fabricated or falsified any idea/data/fact/source in our submission. We understand that any violation of the above will be cause for disciplinary action by the Institute and can also evoke penal action from the sources which have thus not been properly cited or from whom proper permission has not been taken when needed.

(Signature)
Chandrav Jyoti Medhi
200610026016

(Signature)
Shresta Das
200610026051

(Signature)
Shreya Sengupta
200610026052

(Signature)
Subhranil Dey
200610026056

Date: 13 June, 2024

ACKNOWLEDGEMENTS

We would like to express our sincere gratitude to all those who have contributed during this project. This endeavor would not have been possible without their support, guidance, and encouragement.

First and foremost, we would like to express our profound appreciation to Dr. Navajit Saikia, HOD, Electronics and Telecommunication Engineering Department, Assam Engineering College, for providing us with the opportunity to work on the project titled "Design of AlGaN/GaN based HEMT for low-noise and high-speed applications".

We also extend our heartfelt gratitude to our project supervisor, Mr. Niranjan Jyoti Borah, Assistant Professor, Dept. of ETE, for his invaluable mentorship. His expertise, constructive feedback, and unwavering support significantly enriched the quality of our work.

Additionally, we would like to lend our sincere appreciation to our professor, Dr. Bijoy Goswami, Assistant Professor, Dept. of ETE, for supporting us and offering insightful advice.

Finally, we would like to express our gratitude and admiration to our family and friends for voluntarily lending us their skills, experiences, and constant encouragement.

Chandrav Jyoti Medhi (200610026016)

Shresta Das (200610026051)

Shreya Sengupta (200610026052)

Subhranil Dey (200610026056)

ABSTRACT

The High Electron Mobility Transistor (HEMT) is renowned for its exceptional performance, particularly in high-frequency applications, setting itself apart from conventional transistors. HEMTs boast numerous advantages, including significantly faster switching speeds, lower noise levels, and superior high-frequency performance. These features make HEMTs indispensable in contemporary high-speed communication systems and low-noise amplifiers, where maintaining signal integrity and enabling rapid data transmission are critical.

In this project, our focus will be on the design and simulation of an AlGaN/GaN HEMT using the SILVACO TCAD Atlas software. The goal is to optimize the device for high-frequency and low-noise applications. Initially, we will determine the DC characteristics of the HEMT, such as transfer characteristics, drain characteristics, and transconductance, by varying the gate voltage. This will provide a foundational understanding of the device's performance metrics.

After establishing the initial design, we will delve into an extensive analysis of various structural and physical parameters to identify the optimal configuration for our HEMT. Key parameters under investigation will include the doping concentration of the AlGaN layer, the thickness of this layer, the mole fraction of Aluminium within it, and the work function of the gate material. By adjusting these parameters, we aim to achieve several critical objectives: a high cutoff frequency suitable for GHz-range operations, a low threshold voltage to enhance switching efficiency, and high transconductance to improve amplification capabilities.

In addition to these primary performance metrics, we will place a significant emphasis on the noise performance of the HEMT. For low-noise amplifiers, particularly in satellite communication systems, a low noise figure is essential to ensure high signal fidelity.

Furthermore, the effect of temperature on the noise figure will be explored. Understanding how temperature variations impact noise performance is crucial for the reliable operation of HEMTs in different environments. Our findings in this area will be compared with existing research to validate our results and ensure they align with established knowledge.

The comprehensive design and simulation process using SILVACO TCAD Atlas will enable us to optimize the AlGaN/GaN HEMT for high-frequency and low-noise applications. By systematically analysing and fine-tuning the device's structural and physical parameters, we aim to achieve superior performance metrics that meet the demands of modern communication systems. This project will not only contribute to the advancement of HEMT technology but also ensure that our findings are robust and in agreement with prior research in the field. AlGaN/GaN HEMTs are used in various applications due to their exceptional current density and output power. They are poised to become the dominant technology for power electronics and RF/microwave applications. The benefits of using AlGaN/GaN HEMTs include higher power density, higher efficiency, and lower on-resistance compared to traditional silicon and gallium arsenide-based devices. This results in smaller devices, reduced system costs, and increased system efficiency. Additionally, GaN-based devices can operate at higher voltages, reducing the need for voltage conversion and simplifying cooling systems. These advantages make AlGaN/GaN HEMTs suitable for high-power and high-frequency applications in industries such as wireless communication, automotive, and aerospace.

LIST OF FIGURES

LIST OF TABLES

CONTENTS

CHAPTER 1

INTRODUCTION

1.1 Introduction

The project has gone underground to develop new high-performance superconducting high electron mobility transistors (HEMTs) for cutting-edge applications requiring high-speed electronic devices. The project explores the design, simulation, and optimization of this revolutionary HEMT device, studying, analyzing and discussing its DC characteristics and radio frequency applications using the capabilities of Silvaco TCAD (Technical Computer Aided Design) software.

In this chapter we focus on various topics which form the base of the project, and henceforth motivate us to arrive at the desired results of the project. This chapter has been divided into several sections as discussed below.

Firstly, we provide a brief introduction to the area of work and provide insights to various phenomena involved in the background of developing this project. We discuss about heterostructures. Secondly, we list out the researches done in the field of HEMTs and Heterostructures and focused on the shortcomings from where we gained the motivation to carry out our project with proper modifications and advancements.

1.2 Introduction to the area of work

1.2.1 Heterostructures

A semiconductor heterostructure is a sandwich of or junction between two dissimilar semiconductors with different band gaps and a periodic repetition of multiple heterojunctions, is called superlattice. They offer precise control over the states and motions of charge carriers in semiconductors [1] Electrons will flow from higher fermi level (doped layer) to lower fermi level (undoped layer) [3].

The electrons then diffuse from the doped layer into the undoped layer, creating a high concentration of free electrons in a thin region near the interface between the two layers. [2]

This is called Modulation Doping. First proposed by Dingle, Stormer, Gossard, and Wiegmann in 1978, [3] modulation doping in heterostructures is possible because of the dissimilarity in band gap of the materials. It is also possible with Modulation doping to confine electrons at a single interface between an undoped channel material and a doped barrier material. This was achieved both with MBE or MOCVD [4]. Heterostructures are the building blocks of the most advanced semiconductor devices being developed and produced [5].

1.2.2 High Electron Mobility Transistors

HEMT, or High Electron Mobility Transistor, is a form of field-effect transistor, FET, used to provide very high levels of performance at microwave frequencies. It offers a combination of low noise and the ability to operate at very high microwave frequencies. [6]. Therefore, this device is used in areas of RF design that require high performance at very high RF frequencies.

The formation of two-dimensional electron gas (2DEG) is the core component of HEMT. The barrier layer in a HEMT is a wide bandgap material while the buffer layer is composed of a narrow bandgap material. Both these layers may have same n-type doping forming a heterojunction. Generally, the barrier layer has higher doping than the buffer layer. When the barrier layer and the buffer layer are brought in contact with each other, electrons diffuse from wide bandgap material to narrow bandgap material until equilibrium condition is achieved. At equilibrium, the Fermi levels on both the sides get aligned and results in significant band bending. In the channel region, a two-dimensional quantum well is formed due to band bending. The electrons in the channel region are confined to the quantum well thus forming a 2DEG.

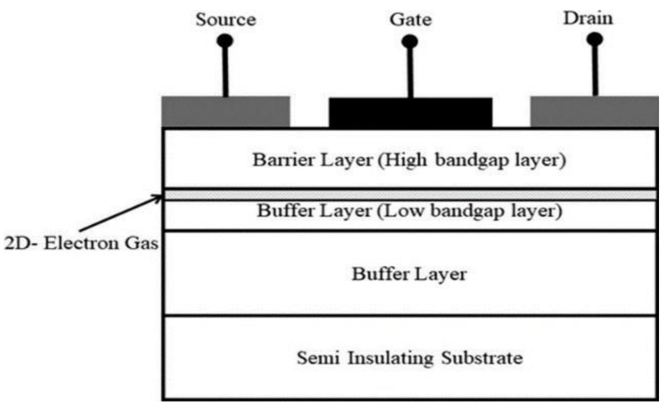

Fig-1.1: Basic cross section of HEMT

The electrons in the channel region are spatially separated from their ionized donor atoms which reduces impurity scattering of mobile charges. Since the 2DEG channel is formed away from the surface, therefore, surface scattering is also reduced. These two phenomena along with an undoped channel improves the carrier mobility in HEMTs. The gate forms a Schottky contact with the barrier layer while drain and source form an ohmic contact with the barrier layer. [6]

1.3 Present-day scenario

The landscape of High Electron Mobility Transistors (HEMTs) has witnessed significant progress in recent years, with a focus on material advancements, device miniaturization, quantum well engineering, and expanded applications in power electronics. The development of a novel normally-off GaN HEMT with high current switching capability (4A) and blocking voltage (600V) by IISc Bangalore represents a significant advancement in power electronics technology. This achievement holds promise for reducing dependence on imported transistors and enabling efficient power conversion in diverse applications, including electric vehicles, locomotives, and high-voltage power transmission and would reduce the cost of importing such stable and efficient transistors required in power electronics [9].

AlGaN/GaN HEMTs exhibit applications in high-frequency power converters, particularly for applications like envelope tracking in radio frequency (RF) transmitters. Here, their ability to handle high frequencies and fast switching can be advantageous. Due to their excellent performance in Low-Noise Amplifiers (LNAs), AlGaN/GaN HEMTs can be integrated into power electronics systems alongside LNAs.

HEMT-based biosensors for the detection of various biomolecules have proved more potential and immense advantages due to their inherent material properties [7]. These recent developments underscore the evolving role of HEMTs in contemporary electronic systems, providing a foundation for future advancements in semiconductor technology.

1.4 Motivation to do the project work

There have been several studies and developments in designing HEMT for low-noise and high-power applications. The main motivation to do the project work is to develop a HEMT to overcome the shortcomings in the previous works done by various scientists and provide a HEMT structure with better noise figure and observe its characteristics for better and advanced applications in the field.

1.4.1 Shortcomings in the previous works

There has been a range of studies on MBE-grown, modulation-doped (MD) heterojunction superlattices of GaAs-$Al_xGa_{1-x}As$, in which low-temperature and room-temperature electron mobilities can be significantly higher than those in equivalent GaAs material grown in other ways where we note that highly anisotropic oscillatory magnetoresistance behavior. There are many papers that report the observation of a two-dimensional hole gas at a semiconductor heterojunction interface. The study showed various shortcomings such as the value of experimental carrier concentration deviated from the low-temperature Hall data. More accurate comparison between theory and experiment will be possible with refined experimental methods and detailed calculations. [8]. Similarly, a range of HEMTs were developed with selectively doped heterojunctions, where substantial improvements in the high-speed capability are expected with improved electron mobilities at low temperatures. [9].

It has been found from several papers that by using proper methods ohmic contact resistance can be reduced. Intrinsic transconductance can be also be improved by increasing doping level or reducing thickness keeping the gate length same [10].

Thus, analyzing the shortcomings encountered in various research papers, we are motivated to move forward with our project and study various aspects of heterostructures and HEMTs.

1.5 Objectives of the work

Problem Statement-1: To investigate about the structure of AlGaN/GaN HEMT

- **Objectives:**
    - To study about the need, advantages, and performance of AlGaN/GaN HEMT from previous researches.

Problem Statement-2: To design and study the characteristics of the proposed structure of AlGaN/ GaN HEMT.

- **Objectives:**
    - To do the DC analysis and find the transfer characteristics, output characteristics and transconductance curve from our proposed structure of AlGaN/GaN HEMT.
    - To study how the characteristics vary with changes in structural parameters and with temperature.

Problem Statement-3: To design and study the characteristics of AlGaN/GaN HEMT for low-noise and high-speed applications.

- **Objectives:**
    - To do the RF analysis of the structure and find out the unity gain cut-off frequency of the device.
    - To find the minimum noise figure of the device.

1.6 Target specifications

The analysis of radio frequency performance of HEMT is essential for analyzing the applications of HEMT which include high-speed and high-power applications for radio communications and other space technologies.

Current semiconductor transistors face limits in terms of energy efficiency, power, bandwidth, and security. To address this, high-quality HEMT with proper structural components are required to adhere the needs of high frequency applications.

HEMTS are widely used in the processing and detection of extremely weak signals, such as quantum computing systems, radio-astronomy, space-science fields and other low noise cryogenic applications [11].

1.7 Organization of the report

The report is organized in different chapters as follows:

- Chapter-1 gives a brief introduction about the area of work. This chapter contains present day scenario, motivation to do the work, objective of the project, target specification and importance of the end result.
- Chapter-2 discusses the literature review. This chapter contains information regarding the project area from various platforms and previous works.
- Chapter-3 discusses the methodologies adopted and tools used to design the structure of the AlGaN/GaN HEMT.
- Chapter-4 discusses the DC analysis of the structure.
- Chapter-5 discusses the structural variation and its effects on the characteristics of the structure.
- Chapter-6 discusses the effect of temperature variation on the characteristics of the structure.
- Chapter-7 discusses the RF analysis of the structure.
- Chapter-8 gives a conclusion to the report including the fields of application and future scopes of improvement.

CHAPTER 2

LITERATURE REVIEW

2.1 Introduction

This chapter aims to establish a foundation for the subsequent discussions by synthesizing and analyzing the current state of knowledge in the field. By examining the works of esteemed scholars and researchers in a chronological manner, this literature review not only contextualizes our study but also lays the groundwork for advancing the discourse in the field.

2.2 Introduction to the project title

The project, “Design of AlGaN-GaN based HEMT for low-noise and high frequency applications” primarily focuses on the unique characteristics of High Electron Mobility Transistors (HEMTs). HEMTs are renowned for their high-speed operation and low noise attributes, making them ideal for high-frequency applications. This project aims to delve deeper into the DC and RF properties, to understand their impact on the performance of HEMTs. The ultimate goal is to design a HEMT that not only operates at high speeds but also to observe any enhancements in the HEMT’s performance due to this addition, thereby pushing the boundaries of what is currently achievable in the field. This literature review will delve into the existing body of knowledge, identify gaps, and set the direction for this groundbreaking research.

2.3 Literature Review

2.3.1 Present state

The current state of High Electron Mobility Transistor (HEMT) technology is quite advanced and promising. Scientists from Bangalore have developed a highly reliable, normally OFF HEMT device that can switch currents up to 4A and operates at 600V. This first-ever indigenous HEMT device made from gallium nitride (GaN) is useful in electric cars, locomotives, power transmission, and other areas requiring high voltage and high-frequency switching. Market for HEMTs is projected to cross the 5 Billion US$ market. GaN HEMTs will acquire a major share of the power device market. With a growing market for electric vehicles in India, such an indigenous development can make India self-reliant for transistor technology [9].

The current research has shifted towards third-generation semiconductors, such as GaN, due to their unique material properties. GaN offers a higher electron saturation drift rate, more robust radiation resistance, and higher thermal conductivity. [12]

2.3.2 Brief background theory

High Electron Mobility Transistors (HEMTs) are field-effect transistors that take advantage of the high electron mobility in a two-dimensional electron gas (2DEG) to achieve high-speed applications. The 2DEG is formed at the interface between two semiconductor materials The larger bandgap material is doped with donor atoms, providing free electrons that are confined to the interface due to the band structure of the materials.
The key to HEMT's high-speed operation is the separation of the conducting 2DEG from the doped layer. This separation minimizes scattering from the ionized donor atoms, allowing the electrons in the 2DEG to move quickly and freely, resulting in high electron mobility.

The DC characteristics of a HEMT, such as the output and transfer characteristics, provide information about the device's static behaviour. The RF characteristics, on the other hand, give insight into the device's high-frequency performance.

2.3.3 Literature Survey

Table-2.1: Literature Review

Ref. No.	**Paper Citation**	**Salient Features**	**Gaps/Future Scopes**
[3]	Dingle, Raymond et al, "**Electron mobilities in modulation-doped semiconductor heterojunction superlattices**", Applied Physics Letters 33, 665-66, 1978	MBE-grown, modulation doped (MD) heterojunction superlattices of GaAs-$Al_xGa_{1-x}As$ has been described, in which low- temperature and room-temperature electron mobilities can be significantly higher than those in equivalent GaAs material grown in other ways. The most important feature of the MD structure is that essentially all of the mobile carriers (electrons confined to the GaAs layer) and their parent donor impurities (in the AlxGa1-xAs layer) are spatially separated from each other in an irreversible manner. The Hall mobilities in the MD structures are as much as a factor of 2 greater than the mobilities of	A range of studies on these new structures is in progress. As an example of the low- temperature behaviour of the 2DEG, we note that highly anisotropic oscillatory magnetoresistance behaviour. At room temperature this may be valuable for a range of device structures, whereas, at temperatures below ~50 K, mobilities of $>10^4$ cm^2 V^{-1} sec^{-1} and electron densities of upto $\sim10^{18}$ cm^{-3} access a new range of

		electrons in uniformly-doped (UD) superlattices or in GaAs of equivalent electron concentration.	fundamental and device possibilities.
[8]	H. L. Störmer, W.-T. Tsang; "**Two-dimensional hole gas at a semiconductor heterojunction interface**." Appl. Phys. Lett. 15 April 1980; 36 (8): 685–687.	This paper reports the first observation of a two- dimensional hole gas at a semiconductor heterojunction interface (GaAs/ AlGaAs). The low temperature experiments yielded a carrier surface density of $7x\ 10^{11}\ cm^{-2}$ and a mobility of $\sim 1700\ cm^2\ V^{-1}\ sec^{-1}$. A scattering time of $\sim 3x10^{-13}$ is obtained.	The value of experimental carrier concentration deviated from the low- temperature Hall data which stated $1.5x10^{12} cm^{-2}$. More accurate comparison between theory and experiment will be possible with refined experimental methods and detailed calculations.
[9]	Takashi Mimura, Satoshi Hiyamizu, Toshiio Fujii and Kazuo Nanbu, **"A New Field-Effect Transistor with Selectively-doped GaAs/n-AlxGa1-xAs Heterojunction"**, Japanese Journal of Applied Physics, Vol. 19, No. 5, May, 1980	A new field-effect transistor, called a high electron mobility transistor (HEMT), with selectively doped GaAs/n- $Al_xGa_{1-x}As$ heterojunctions was described. 77K and 300K mobilities of the HEMT are significantly higher than those of GaAs MESFET with similar drain saturation current. Dramatic increase in transconductance of the HEMT has been observed when the HEMT was cooled to 77K. Crude estimation showed that the high-speed performance of the HEMT should be 3 times superior to that of the MESFET at 77K.	Further substantial improvements in the high- speed capability of the HEMT are expected with improved electron mobilities at low temperatures.
[13]	K. Y. Cheng, A.Y. Cho, T.J. Drummond, H. Markoc; **"Electron mobilities in modulation doped Ga0.47In0.53As/ Al0.48In0.52 As heterojunctions grown by molecular beam epitaxy"** Appl. Phys. Lett. 15 January 1982; 40(2): 147–149.	Modulation doped $Ga_{0.47}In_{0.53}As$-$Al_{0.48}In_{0.52}As$ single-period heterostructures have been prepared by molecular beam epitaxy (MBE). In order to reduce the coulombic interaction between the ionized impurity atoms and the conduction electrons, a thin layer of undoped $AI_{0.48}In_{0.52}As$ (about 80 Å) was grown at the $Ga_{0.47}\ In_{0.53}$ As -$Al_{0.48}In_{0.52}As$ interface. Electron mobilities as high as 8915 cm^2 /Vs at 300 K, 60 120 cm^2/V s at	Improvement in the growth of pure $Ga_xIn_{l-x}As$ epitaxial layers will increase the electron mobilities of the modulation doped heterostructures. Parameters such as layer thickness, carrier concentration, and the width of the thin undoped region could be optimized

		77 K, and 90420 cm^2/V s at 10 K were obtained with an average electron concentration of ~ $10^{17}cm^{-3}$.	
[10]	Chen, C.Y. & Cho, A.Y. & Cheng, Kuei-Yueh & Pearsall, Thomas & O'Connor, P. & Garbinski, P.A. (1982). "**Depletion mode modulation doped al0.48in0.52as-ga0.47in0.53as heterojunction field effect transistors**", Electron device letters. 152-155.	First demonstration of depletion mode modulation doped $Ga_{0.47}In_{0.53}As$ field effect transistor. DC transconductances of 31 mmho/mm at 300 K and 69 mmho/mm at 77 K have been measured for device with gate length 5.2 um and gate width 340 um. Source resistances of the FET is estimated to be 22 ohms at 300K and 10 ohms at 77 K. Intrinsic transconductances of 41 mmho/mm at 300 K and 89 mmho/mm at 77 K have been calculated. High contact resistances of 6.4 ohm-mm at 300K and 2.9 ohm-mm at 77K have been observed for ohmic contacts. It is caused by oxidation of the top $A1_{0.48}In_{0.52}As$ layer.	Ohmic contact resistance can be reduced by growing a thin Ga 0.47 In 0.53 As layer on top of the Si- doped Al 0.48 In 0. 52 As layer to prevent the Al 0.48 In 0.52 As layer from oxidation. Intrinsic transconductance can be improved by reducing the thickness of $Al_{0.48}In_{0.52}As$ layer and increasing the doping level of the $Al_{0.48}In_{0.52}As$ layer keeping the gate length same. Significant improvement in the device characteristics is expected by reducing the thickness of the Al0.48In0.52As as well as the $Ga_{0.47}In_{0.53}As$ layers and by improving the ohmic contacts.
[14]	Chin-An Chang, L. L. Chang, E. E. Mendez, M. S. Christie, L. Esaki; **"Electron densities in InAs–AlSb quantum wells",** J. Vac. Sci. Technol. B 1 April 1984; 2 (2): 214–216.	Both single wells and super- lattices of InAs-AlSb have been grown by molecular beam epitaxy on GaAs substrates. The InAs layer thickness ranged from 50 to 300 Å, and the AlSb layer thickness was 200 Å in the SW and 100 Å in the superlattices. A top layer of 100Å GaSb was used to protect the AlSb layers from reacting with air. For the cleaved samples, both the electron densities and mobilities increase with the InAs layer thickness for the SW structures. The superlattices show a similar increase in electron densities but	The chemical process for the creation of the donors was not known. The results were too scattered to draw definitive conclusions

		exhibit higher mobilities than those in the SW structures, particularly for thin layers. For the etched samples, the measured electron densities are significantly higher, scattering around $2x10^{12}$ cm^{-2} and are independent of the layer thickness. The mobilities, on the other hand, agree with those obtained from the cleaved samples for the same layer thickness.	
[15]	H. L. Störmer, K. Baldwin, A. C. Gossard, and W. Wiegmann, **"Modulation doped field effect transistor based on a two- dimensional hole gas",** Applied Physics Letters 44, 1062 (1984);	First demonstration of p-type MODFET with 2D hole gas. Carrier confining valence band discontinuity for 2D hole is = ~100meV, carrier concentration of p = $6.1x10^{11}cm^{-2}$, mobility = $32000cm^2/Vs$ at 4.2K and p = $6.3x10^{11}$ cm^{-2}, mobility = $3900cm^2/Vs$ at 77K. Gate capacitance = $1.6x10^{-7}$F/cm2. Pinch-off Voltage= 350mV at 77K, 250mV at 4.2K. Leakage current is < 100pA. Transconductance at zero gate voltage is 7.1mS at 77K, 11.1mS at 4.2K, channel resistance = 75ohm and 10ohm respectively.	Contact resistance can be improved, Predicted 18ohm and 10ohm at 77K and 4.2K. Light sensitivity of the p contacts has to be eliminated. Pinch-off voltage is not the same as predicted to be 610mV at 4.2K. Difficult to account for the temperature dependence of pinch- off voltage.
[16]	D. V. Lang, R. People, J. C. Bean, A. M. Sergent; "**Measurement of the band gap of GexSi1−x/Si strained-layer heterostructures**", Appl. Phys. Lett. 15 December 1985; 47 (12): 1333–1335.	Leakage current is < 100pA. Transconductance at zero gate voltage is 7.1mS at 77K, 11.1mS at 4.2K, channel resistance = 75ohm and 10ohm respectively. doping effect in Si/Ge0.2 Si0.8 heterojunctions grown by molecular beam epitaxy. Peak hole mobilities of - 3300 cm^2 V^{-1} s^{-1} have been observed at 4.2 K. Two-dimensional nature of the hole gas and yield a surface carrier density of $3.5x10^{11}$ cm^{-2}, carrier mass m* = ~0.30± 0.02mo at Ho = 35Kg. Using the SdH carrier mass m* = 0.30mo we derive a	Identical measurements on n-type heterojunctions having the same Ge content (x=0.2) have failed to show a sustained enhancement of mobility at low temperatures, indicating that ▽Ev >▽Ec. If, however, we assume gs= 1 in the high field regime, then the SdH value of ns is unchanged and the low field data could be explained in terms of an unresolved spin splitting. At present these results

		Fermi energy EF~3 meV and a scattering time ~ 6 x 10-13 s for the 2DHG. (G means Gauss. 1G=10-4 Tesla)	are not clearly understood.
[17]	A. Ketterson, M. Moloney, W. T. Masselink, C. K. Peng, J. Klem, R. Fischer, W. Kopp and Hadis Morkoc, "**High Transconductance InGaAs/AlGaAs Pseudomorphic Modulation-Doped Field-Effect Transistors**", IEEE Electron Device Letters, Vol. EDL-6, No. 12, December, 1985	MODFET using the InGaAs/GaAs system has been introduced where a thin layer of InGaAs is sandwiched between an undoped GaAs buffer layer and a doped GaAs cap layer. $In_{0.15}Ga_{0.85}As/Al_{0.15}Ga_{0.85}As$ modulation-doped field effect transistors (MODFET's) exhibiting extremely good dc characteristics have been successfully fabricated. Preliminary microwave measurements indicate a 300 K current gain cut-off frequency of about 20 GHz, which is 25 percent higher than comparable GaAs/AlGaAs MODFET's.	Compared to a study done in 1988 [41], they developed devices with 0.15-0.25-um gate length have room temperature drain currents as high as 600 mA/mm and room temperature transconductance as high as 500 mS/mm.
[18]	Abstreiter G, Brugger H, Wolf T, Jorke H, Herzog HJ. **"Strain-induced two-dimensional electron gas in selectively doped Si/SixGe1-x superlattices",** Phys Rev Lett. 1985 Jun 3;54(22):2441-2444.	This paper reports on the observations of the two-dimensional nature of electron gases and of mobility enhancement in selectively doped Si/Si_xGe_{1-x} strained- layer superlattices. The effect of electron mobility enhancement due toselective doping is only achieved when the Si_xGe_{1-x} layers are doped. The oscillation period observed with the magnetic field perpendicular to the layers leads to a two-dimensional electron density, $n_s = (1.54 \times 10^{12})\, g_v\, cm^{-2}$/layer; g_v is the valley degeneracy. With the assumption g_v=2, the resulting, $n_s = 3.08 \times 10^{12}\, cm^{-2}$ is in reasonable agreement with the total density obtained from Hall measurements, which gives $N_s = 4 \times 10^{13}\, cm^{-2}$ for the ten layers.	Samples used for this investigation were not optimized for maximum mobility. Improvements can be made by increasing the space thickness, by lowering the carrier concentration, and by lowering the background impurities
		This paper describes the first successful fabrication of n-channe1 modulation doped $Si_{0.5}Ge_{0.5}/Si$ FET. The device gate length and width are 1.6 and 160um respectively. Drain	The buffer layer may be improved with respect to its background doping. The undoped silicon layer forming the abrupt

[19]	H. Daembkes, H.-J. Herzog, H. Jorke, H. Kibbel and E. Kasper, "**The n-channel SiGe/Si Modulation doped field effect transistor**" in IEEE Transactions on Electron Devices, vol. 33, no. 5, pp. 633-638, May 1986	to source spacing is taken equal to 5um. Threshold voltages around -1.9 and -0.9V are achieved for devices with sheet carrier concentration of $3.6x10^{11}$ cm^{-2} and $1x10^{11}$ cm^{-2} respectively. The best values of the extrinsic transconductance are 40 mS/mm for the 1.6-um devices. At room temperature the mobility profile shows very high mobility values of up to 1550 cm^2/Vs near the hetero-interface. The maximum carrier concentration of $2x10^{18}$ cm^{-3} is observed exactly at the position of the $Si_{0.5}Ge_{0.5}/Si$ hetero-interface.	heterojunction has to be optimized in thickness and in background doping. The Si1-xGex-layer has to be optimized with respect to nearly all its parameters. Further modifications of the device structure are possible
[20]	Fritz, Ian J. et al. "**Influence of built-in strain on Hall effect in InGaAs/GaAs quantum well structures with p-type modulation doping**." Applied Physics Letters 49 (1986): 581-583.	Studied the Strain effect using Hall data between 4K and 300K. For all samples, transport is dominated by carriers with a single, well defined hole mass. Energy separation of the ground-state levels of the two sets of quantum wells is small (perhaps ~ 10 meV). At 77 K the most important scattering mechanism is expected to be acoustic phonon scattering. In two dimensions, the acoustic mobility goes as the inverse square of the effective mass. From a mass ratio of 0.35:0.15 they expect a mobility ratio of ~ 5.4, in good agreement with the observed ratio of 4.7. In contrast to the AIGaAs results, the high-temperature activation process depends strongly on the strain built into the quantum wells. Main conclusion - the built-in strain in p-type InGaAs/GaAs quantum well structures has a large, direct effect on electrical transport at all temperatures from 4 to 300 K. At the higher temperatures an activation process is observed which appears clearly correlated with the magnitude of the strain- induced valence-band splitting.	The Hall mobility is expected to depend on other factors in addition to the built-in strain, including the carrier density and the alloy composition. Variations in these quantities probably account for a significant amount of the scatter in the data, but are not large enough to obscure the main trend of the results.

		The 77 K Hall mobility increases by a factor of - 5 as the compressive planar strain is increased from 0.5 to 1.4%, suggesting the possibility of enhanced performance for low temperature devices such as p-channel field-effect transistors.	
[21]	Razeghi, Manijehet al. **“First observation of two-dimensional hole gas in a Ga0.47In0.53As/ InP heterojunction grown by metalorganic vapor deposition.” Jour nal of Applied Physics 60 (1986): 2453-2456.**	Their low-temperature magneto transport measurements demonstrate the two-dimensionality of the system and yield a total hole density at the interface of = $7.6x10^{11}$ cm^{-2} and a Hall mobility = 10500 cm^2/Vs was reached at 4.2 K. Angle-dependent Shubnikov- de Haas measurements as well as quantized Hall effect observations confined the two-dimensionality of the system. In contrast to the case of the 2D hole gas in GaAs/ AIGaAs, low-temperature persistent photoconductivity was observed, significantly increasing the hole density at the interface. Carrier concentration= 2.16x 1011/cm2. Channel hole mobility to be 2377 cm^2/Vs. A very high transconductance of 89 mS/mm at 77 K has been achieved.	The accessible magnetic field ranging up to 18T is not sufficient to observe the minima corresponding to two partially filled and one entirely filled Landau levels and to determine the high-field.
[22]	Pearsall, Thomas& Bean, J. (1986). **“Enhancement and depletion- mode p-channelGe(x)Si(1-x) modulation- doped FET's”.** IEEE Electron Device Letters - IEEE ELECTRON DEV LETT. 7. 308-310.	They reported enhancement- and depletion-mode p- channel modulation-doped field-effect transistors (FET’s) in Si. Si/Ge_xSi_{1-x} heterostructures grown by molecular-beam epitaxy (MBE) with one- dimensional confinement of holes at the heterostructure interfaces. Transconductances of 2.5 and 3.2 mS/mm were measured at300 K for enhancement- and depletion-mode devices, respectively at Vt = + 5 V. The relatively high source resistance is related to the mobility of holes (80 cm^2/Vs in GexSi1-x), the long source drain spacing (8um), and a low sheet charge in the channel	Much work still needs to be done to control the threshold voltage, to improve passivation techniques, and to reduce parasitic resistances. The measured source resistance in their devices is 60 0-mm, and degrades the transconductance by about 30 percent.

		region ($2.5x10^{11}cm^{-2}$). The mobility and sheet charge were determined directly by Hall effect measurements.	
[23]	P.C. Chao, P.M. Smith, K.H.G. Duh, J.M. Ballingall, L.F. Lester, B.R. Lee, A.A. Jabra (Electronics Laboratory, General Electric Co., Syracuse, NY 13221), and R.C. Tiberio (National Nanofabrication Facility, Cornell University, Ithaca, NY 14853), **"High Performance 0.1um Gate- Length Planar- Doped HEMTs"**, IEEE, 1987	AlGaAs/InGaAs/GaAs planar-doped pseudomorphicHEMTs with a gate length of 0.1um have been successfullyfabricated. Due to the quantum-well channel structure, the InGaAs pseudomorphic HEMT has improved carrier confinement and therefore a reduced short channel effect. The pseudomorphic HEMT also provides very high electron velocity and sheet charge density due to the superior carrier transport properties in the InGaAs channel and the large conduction band discontinuity with AlGaAs. The performance of the planar-doped HEMTs is superior to that of the uniformly-doped HEMT. The 0.1um gate structure of planar-doped devices, however, has a very high parasitic resistance of ~1700 ohm/mm (DC, end-to-end). This resistance value is 20 times higher than that of the 0.25um T-shaped gate. In spite of the extremely high parasitic gate resistance, low noise figures were measured with very high associated gains for the devices.	The results clearly demonstrate the potential of the extremely-short gate length planar-doped pseudomorphic HEMTs for millimetre-wave applications. Further improvementsin device performance can be achieved through a reduction of gate resistance.
[24]	Lee, Chien-Ping et al. **"High-transconductance p-channel InGaAs/AlGaAs modulation-doped field effect transistors."** IEE E Electron Device Letters 8 (1987): 85-87.	With a 1-pm gate, the device exhibits transconductances of 17.8 and 89 mS/mm at room temperature and 77 K, respectively. Experimental results indicate an extrinsic transconductance greater than 200 mS/mm is achievable with reduced ohmic contact resistance and gate leakage. With the measured K factor of 400 mS/V mm (at 77 K), they calculated	Contact resistance of 0.5 ohm should be achievable if the proper metallization procedure is used. If the source resistance can be reduced to 1 ohm.mm, an extrinsic transconductance of above 200 mS/mm at 77 K will be achieved with our current layer structure. This mobility

		the channel hole mobility to be 2377 cm2/Vs.	value is less than what is expected from this material system based on Hall measurements.
[25]	M. D. Feuer et al., **"InP-based HIGFETs for complementary circuits,"** in IEEE Transactions on Electron Devices,vol. 36, no. 11, pp. 2616-, Nov. 1989	They reported the first p- channel heterostructure FET's fabricated on InP substrates, as well as advanced results on submicrometer n-channel HIGFET's. It provides a nearly-ideal separation of about 0.5 V between p- and n-channelthresholds. P-HIGFET's with 1-pm gate length were made using lattice-matched InGaAs channels and InAlAs barriers. A typical device shows sharp pinch-off, with threshold voltage of -0.59 (-0.40) V, transconductance of 26 (8) mS/mm, and K-value of 48 (12) mS/V-mm, measured at a temperature of 82 (290) K. Microwave characterization of several n-HIGFET wafers with L, down to 0.3 pm yields f, up to 115 GHz, corrected for pad capacitance, with an effective drift velocity of 2.0×10^7 cm/s.	Limitations due to parasitic source resistance and gate leakage current. Early results show that high-performance complementary circuits on InP substrates should be possible with realistic advances in today's technology.
[26]	U. K. Mishra et al., **"Impact of buffer layer design on the performance of AlInAs-GaInAs HEMTs,"** in IEEE Transactions on Electron Devices,vol. 36, no. 11, pp. 2616-, Nov. 1989	They reported on a study of buffer layer design on the characteristics of $Al_{0.48}In_{0.52}As$-$Ga_{0.47}In_{0.53}As$ HEMT's. The aim of the study is to understand and correct the problem of high output conductance observed in devices with a high transconductance. The device with the standard undoped AlInAs buffer had a g_m of 580 mS/mm with an output conductance g_o of 27 mS/mm. The resultant low- frequency voltage gain g_m/g_o was 21.5. The device with the p-type AlInAs buffer layer exhibited a g_m of 540 mS/mm with g_o of 20 mS/mm. The voltage gain was, therefore, 27.	Substantial g_m compression was observed toward pinch-off caused by a combination of residual donors in the GaInAs buffer and substrate injection over the slightly lower confining barrier.

		The device with the p-type GaInAs buffer had a g_m of 550 mS/mm and a g_o of 25mS/mm with a resultant voltage gain of 22. Lastly, the device with the low-temperature AlInAs buffer had a g_m of 550 mS/mm and a g_o of 15 mS/mm with a voltage gainof 36.7	
[27]	L. F. Lester et al., **"High-efficiency 0.25- um gate-length pseudomorphic power heterostructure FETs at millimeter-wave frequencies,"** in IEEE Transactions on Electron Devices, vol. 36, no. 11, pp. 2616-2617, Nov. 1989	They have measured a maximum 35-GHz power added-efficiency and powerdensity of 49 percent and 0.94 W /mm, respectively, for the DCHMODFET; 43 percent and 0.97 W/mm for the DHHEMT; 32 percent and 0.75 W/mm for the HEMT; and 31 percent and 0.77 W/mm for the DCHFET. The DCHFET has doping only in the quantum well. The purpose of the comparison study is to determine whetherany one of these four devices is noticeably superior in terms of efficiency and/or power density at millimeterwave frequencies.	The power performance and efficiency of the DCHFET was low.
[28]	W. Hansen, T. P. Smith, J. Piao, R. Beresford, W. I. Wang; **“Magnetoresistance measurements of doping symmetry and strain effects in GaSb-AlSb quantum wells.”** Appl.Phys. Lett. 1 January 1990; 56 (1): 81–83.	Made the first magneto transport measurements of two- dimensional holes confined to GaSb in modulation-doped AlSb/GaSb heterostructures. The multiple quantum well samples had a low temperature (4.2 K) mobilityof 9000 cm^2/Vs and a per-layer carrier density of 1.4 x 10^{12} cm^{-2}. The asymmetric single quantum well sample had amobility of 15000 cm^2/Vs and a carrier density of $1.05x10^{12}$ cm^{-2}.	At high magnetic fields, the Hall voltage shows strong deviations from linear behavior, but they do not see good quantization of the Hall voltage below 9T, even at fairly low temperatures (0.4 K)
[29]	L. F. Luo, K. F. Longenbach and W. I. Wang, **"p-channel modulation- doped field- effect transistors**	They reported the successful operation of the first AlSbAs/GaSb p-channel modulation-doped field-effect transistor. Devices with 1-um gate length exhibit transconductances of 30 and 110 mS/mm at room temperature and 80 K, with respective maximum	

	based on AlSb0.9As0.1/GaSb," in IEEE Electron Device Letters, vol. 11, no. 12, pp. 567-569, Dec. 1990	drain current densities of 25 and 80 mA/mm. The low field Hall mobility and sheet carrier density of this modulation doped structure are 260 cm2/Vs and 1.8 x 1012 cm-2 at room temperature and 1700 cm2/V s and 1.4 x 1012 cm-2 at 77 K.	
[30]	M. Asif Khan, J. N. Kuznia, J. M. Van Hove, N. Pan, J. Carter; **"Observation of a two- dimensional electron gas in low pressure metalorganic chemical vapor deposited GaN-AlxGa1−xN heterojunctions**". Appl. Phys. Lett. 15 June 1992; 60 (24): 3027–3029.	This paper confirmed the presence of a two- dimensional electron gas (2DEG) in a wide band-gap GaN-AlxGa1-xN heterostructure sample grown using low pressure MOCVD. The 2DEG mobility for a GaN-Al0.13Ga0.87N heterojunction was measured to be 834 cm2 /V s at room temperature. It monotonically increased and saturated at a value of 2626 cm2 /V s at 77 K. The 2DEG mobility remained nearly constant for temperatures ranging from 77 to 4.2 K. The two-dimensional carrier concentration was estimated to be 1×10^{11} cm-2. The peak mobility for the 2DEG was found to decrease with the heterojunction aluminum compositions in excess of 13%.	Deposition of high quality, undoped, low carrier density AlxGa1-xN was not possible leading to discrepancy in sheet carrier density determination. Factors such as strain due to lattice mismatch can be responsible for the mobility degradation. Further research is required to understand this behaviour.
[31]	M. Asif Khan, A. Bhattarai, J. N. Kuznia, D. T. Olson; **"High electron mobility transistor based on a GaN-AlxGa1−xN heterojunction." Appl. Phys. Lett. 30 August 1993; 63 (9): 1214–**	This paper studied the fabrication and dc characterization of a high electron mobility transistor (HEMT) based on a n-GaN-Al0.14Ga0.86N heterojunction. The structure of HEMT consisted of a 0.6 um-thick n-GaN channel with a l000- Å-thick cap layer of n-type Al0.14Ga0.86N and a sapphire substrate. Room-temperature transconductance of 28 mS/mm was measured for a device with a 10um channel opening and a gate length	HEMT devices, but does not investigate the AC characteristics, such as the frequency response, the noise figure, the power gain, or the linearity and also does not consider the effects of parasitic elements, such as the gate resistance, the source and drain resistances, the gate capacitance, or the substrate capacitance, on the device

	1215.	and width of 4 and 50um, respectively (gate voltage +0.5 V). This increases to a value of 46 mS/mm at 77 K. Sheet carrier density was measured to be 1.15x1013 cm^{-2} at 300K and $7.6x10^{12}$ at 77K. The carrier mobility was found to be 563 cm^2 V-1s-1 at 300K and 1517 cm^2 V-1s-1 at 77K.	performance.
[32]	Klem, J.F., Lott,J.A., Schirber, J.E. et al. **“Strained quantum well modulation- doped InGaSb/AlGaSb structures grown by molecular beam epitaxy.”** J. Electron. Mater. 22, 315–318 (1993)	Advances in the growth ofantimony-containing III-V compound semiconductorshave been motivated for improved performance. Of particular interest for field-effect transistor devices is the nearly lattice-matched GaSb/InAs/AlSb system, where both InAs n-channel, and GaSb p-channel transistors have been demonstrated as the basis fora complementary logic technology. Field-effect transistors fabricated in the InGaSb/AlGaSb system exhibit excellent performance at both 300 and 77K. Demonstrated improved low- field mobilities and reduced hole masses in modulation- doped p-type A1GaSb/In0.25 Ga0.25Sb structures compared to AlGaSb/GaSb designs. Hole masses as light as 0.071 o and 77K mobilities as high as 7000 cm2/Vs have been demonstrated.	The performance of these devices appears to be limited by the relatively low Schottky barrier height associated with the use of AlGaSb as the barrier material. Improvements in the device structure and fabrication process are expected to result in further enhancement of device performance.
[33]	Loren Pfeiffer, K.W. West (Bell Laboratories, Lucent Technologies, Inc., Murray Hill, NJ 07974, USA), **“The role of MBE in recent quantum Hall effect physics discoveries”,** Physica E, Elsevier B.V, 2003	Some of the physics issues are discussed that are encountered in maintaining the heterostructural quality as the electron density ∗ Corresponding author. approaches the extremes of this range, and will review some recent Quantum-Hall-Effect (QHE) experiments where the sample mobility has had an especially significant impact.	The temperature of the electrons should be lowered to 1mK and below. The samples shouldhave high mobility. There must be a better quantitative handle on the nature of sample disorder has each imperfection in the sample can affect the

			mobility in a different manner.
[34]	Umansky, Vladimir & Heiblum, M. & Levinson, Y. &Smet, J. & Nübler, J. & Dolev, Merav. (2009). **“MBE growth of ultra- low disorder 2DEG with mobility exceeding 35x10^{6} cm^{2}/V s.”** Journalof Crystal Growth. 311. 1658-1661	This demonstrates the MBE growth of AlGaAs/GaAs heterostructures using a short- period superlattice (SPSL) doping instead of the more standard n-AlGaAs doping. Such doping process allows the use of a low AlAs mole fraction spacer which, in turn, leads to a lower background of impurities as well as a better interface quality. Mobility exceeding 35x10^{6} cm^{2} /V s was measured in samples with doping introduced on both sides of a quantum well (QW). It shows the developing of an alternative doping scheme in AlGaAs/GaAs modulation- doped structures, which allows obtaining both extremely high electron mobility without illumination and facilitating the fabrication of mesoscopic devices with relatively stable gate behaviour.	Neither the low-field mobility (as high as 36x10^{6} cm^{2} /V s) nor the quantum lifetimes (around 15 ps) were found to be relevant parameters that predict the quality of the FQHE states. Experiments in which the amount of over-doping was altered suggested that the disorder landscape generated by the RI impurities affects strongly the appearance of the FQHE.
[35]	del Alamo, Jesus A. **"The High-Electron Mobility Transistor at 30: Impressive Accomplishment s and Exciting Prospects".** 2011 International Conference on Compound Semiconductor Manufacturing Technology, May16-19, 2011, Indian Wells, California	This review paper discussed the evolution of HEMT. The HEMT was based on theconcept of modulation doping. A modulation-dopedstructure creates a two- dimensional electron gas at the interface between two semiconductors of different bandgaps. Atomic layer precision growth capabilities are made possible by molecular beam epitaxy. The high mobility and highly confined nature of the two-dimensional electron gas suggested that modulation doping could be exploited to make high-speed field-effect transistors.	Future generation ultra-dense chips will demand significant operating voltage reductions. AlGaAs/GaAs structures will result in new insights. Lighter, more efficient and more reliable radar and communication systems using GaN. Antimonides will soon emerge into the real world and enable a new generation of ultra-low power and high-speed systems.

2.4 Theoretical discussions

The invention of the high-electron- mobility transistor (HEMT) is usually attributed to physicist Takashi Mimura, while working at Fujitsu in Japan. The basis for the HEMT was theGaAs (gallium arsenide) MOSFET which Mimura had been researching as an alternative to the standard silicon (Si) MOSFET since 1977 [9]. The key element that is used to construct an HEMT is the specialized PN junction. The most common materials used Aluminium Gallium Nitride (AlGaN) and Gallium Nitride (GaN). Its principle is based on a heterojunction which consists of at least two different semiconducting materials brought into intimate contact. Because of the different band gaps and their relative alignment to each other, band discontinuities occur at the interface between the two semiconducting materials. These discontinuities are referred to as the conduction and valence band offsets. By choosing proper materials and compositions thereof, the conduction band offset can form a triangular shaped potential well confining electrons in the horizontal direction. Within the well the electrons can only move in a two-dimensional plane parallel to the hetero-interface and are therefore referred to as a two-dimensional electron gas (2DEG). The electrons in the channel of a HEMT are able to move very quickly because of the high mobility of the semiconductor material. This means that the device can switch on and off very quickly. It offers low noise figure, high sensitivity and very high levels of performance at microwave frequencies. It is also possible with modulation doping to confine electrons at a single interface between an undoped channel material and a doped barrier material. This was achieved both with MBE or MOCVD [4]. Molecular beam epitaxy is probably the most popular Si/SiGe growth method in academia and research labs. MBE is generally a physical-vapor deposition process, where the growth of the film is by direct co-evaporation of silicon and germanium (from ultra-pure solid sources), together with the desired dopants under ultra-high vacuum (UHV) conditions. One of the earliest published studies on the use of the MBE method for single crystal film growth was that of Joyce and Bradley. In the mid-1960s they grew homoepitaxial layers of Si from SiH4. The growth rates were very low comparative to other Si film methods and therefore not competitive in a market that needed 10 um-thick films. The discussions so far have primarily focused on the theoretical facets of AlGaN/GaN HEMTs. However, it’s crucial to acknowledge that there are numerous practical engineering hurdles to overcome, including improving material quality, refining device fabrication methods, and mastering interface engineering, to truly harness the potential of AlGaN/GaN HEMTs. Despite these challenges, the benefits of AlGaN/GaN HEMTs promises for the development of high-performance transistor devices.

2.5 Conclusion

In conclusion, the literature review has provided a comprehensive exploration of the subject matter. Through an extensive and detailed analysis of existing research, we have gathered and examined crucial information related to the project. This thorough examination has shed light on the current state of knowledge within the field, providing a clear understanding of what has already been studied, established, and agreed upon by scholars. The review process has also been instrumental in identifying gaps in the current research. These gaps represent areas where information is either insufficient, outdated, or entirely lacking, highlighting the limitations of the existing body of knowledge. Recognizing these gaps is critical, as it underscores the areas that need further exploration and research. Furthermore, the literature review has highlighted specific areas that warrant additional investigation. By pinpointing these areas, we can direct future research efforts more effectively, ensuring that new studies address the deficiencies identified and contribute to a more comprehensive and nuanced understanding of the subject. This targeted approach not only helps in filling the existing gaps but also in advancing the field by exploring new dimensions and perspectives.

CHAPTER 3
METHODOLOGY

3.1 Introduction

This chapter deals with the methodologies adopted in this project. This chapter contains information about the software used and the device parameters adopted for the formation of the proposed structure of the AlGaN/GaN based HEMT for our project.

3.2 Software Tool Used

This is a simulation-based project and the software tools that we have used is SILVACO ATLAS TCAD Tool. Technology Computer-Aided Design or TCAD refers to the use of computer simulations to develop and optimize semiconductor process technologies and devices. TCAD is a branch of electronic design automation. It models semiconductor fabrication and device operation. Modelling of the fabrication is called Process TCAD and modelling of the device operation is called Device TCAD. The advantages of using this tool is that it reduces development cost and shorten the development time. The simulation of the device is done by ATLAS Tool. It provides physics based simulation of the semiconductor device whose physical structure and bias conditions are specified. It includes material 15 properties for the commonly used semiconductor materials. The DeckBuild tool is the editor for SILVACO and it interface is shown in Fig-3.1. It is used to write the codes and then to simulate them. The code files are of three types. They are:

- ".in file" is basically the main editable file
- ".str file" comprises the information about the structure
- ".log file" it comprises of all the electrical information and calculated parameters after the simulation.

The result outputs are viewed in the tool named Tonyplot. It is a graphical post processing tool to use with all the SILVACO simulator. It shows the results as structure file or log file.

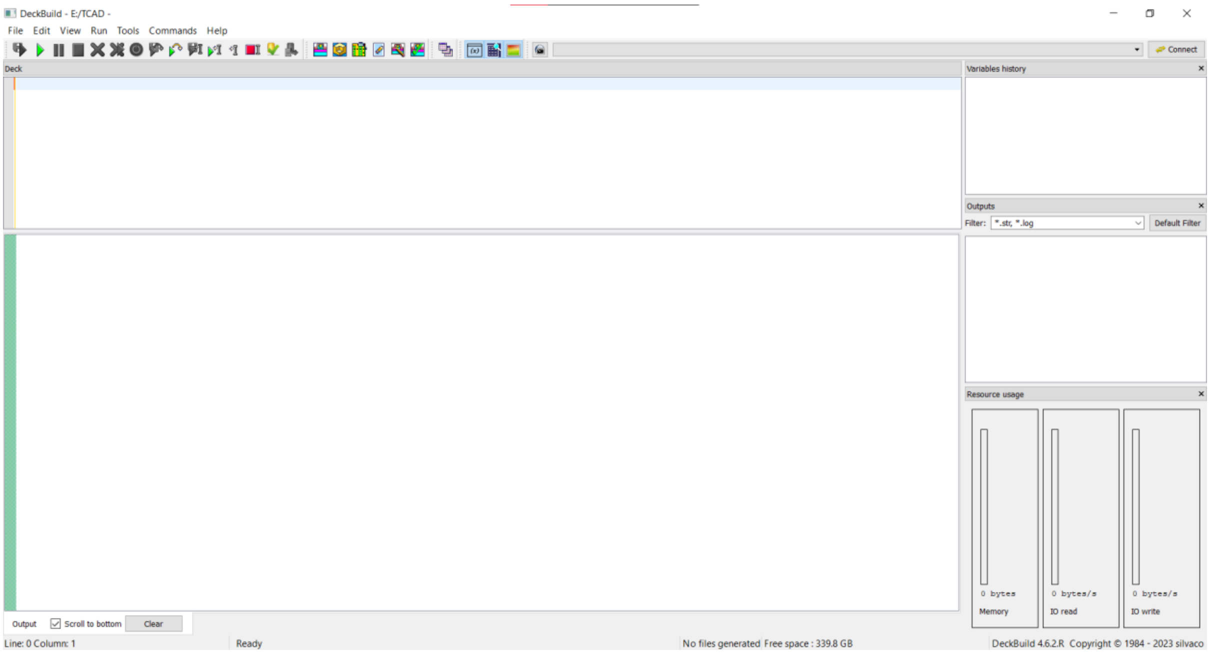

Fig-3.1: Deckbuild interface

3.3 Device Specification

Taking the references from [8, 39, 40], we have proposed a structure of AlGaN/GaN HEMT on SiC substrate, including an AlN nucleation layer. This nucleation layer is used to overcome the lattice mismatch and facilitate the growth of the GaN layer over the SiC substrate. SiC as a substrate provides excellent thermal conductivity and is beneficial for effective heat removal in high power applications. The device parameters for the proposed structure is given in Table-3.1, and the structure is shown in Fig-3.2.

Table-3.1: Device parameters for proposed structure of AlGaN/GaN HEMT

Material	**Thickness (in nm)**
$Al_{0.23}Ga_{0.77}N$	25
GaN	1500
AlN nucleation layer	25
SiC substrate	850

In our proposed structure, we have used Gold as the gate material having work function of 5.1eV and gate length 1um. The channel is formed by the highly n-doped AlGaN layer with 23% Al and 77% GaN.

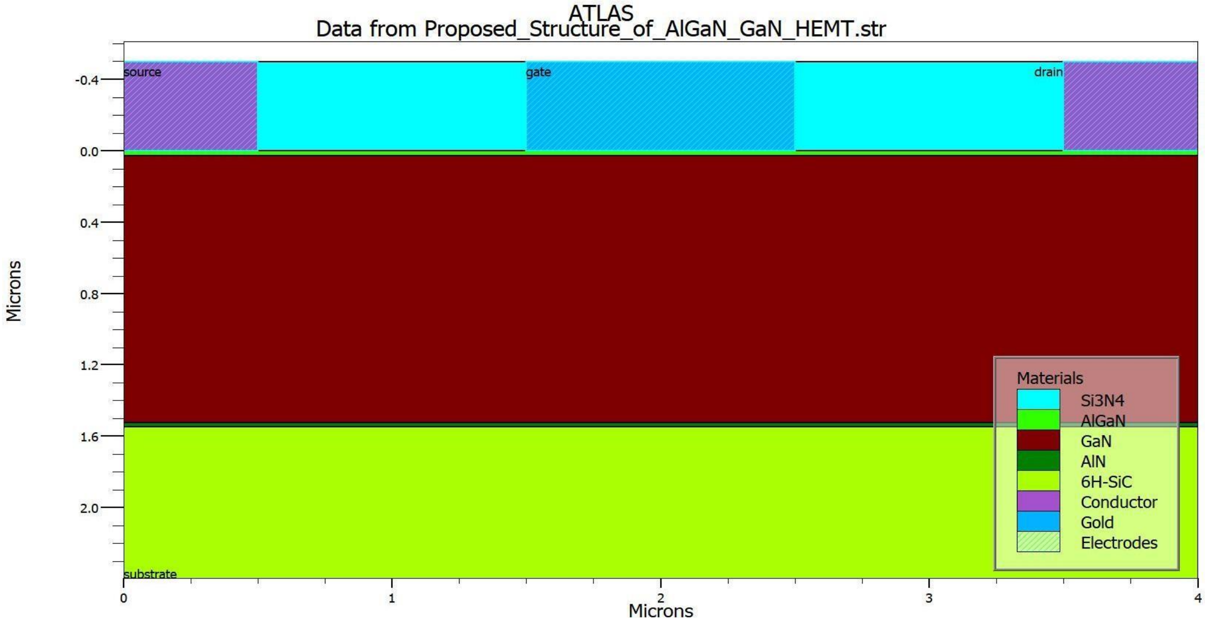

Fig-3.2: Proposed structure of AlGaN/GaN HEMT device

The structure meshing is defined in such a way that the mesh is fine in the channel and near the interface of the different layers, where a change occurs in the material properties, like doping concentration and energy bandgap. The mesh structure of the proposed structure is shown in Fig-3.3.

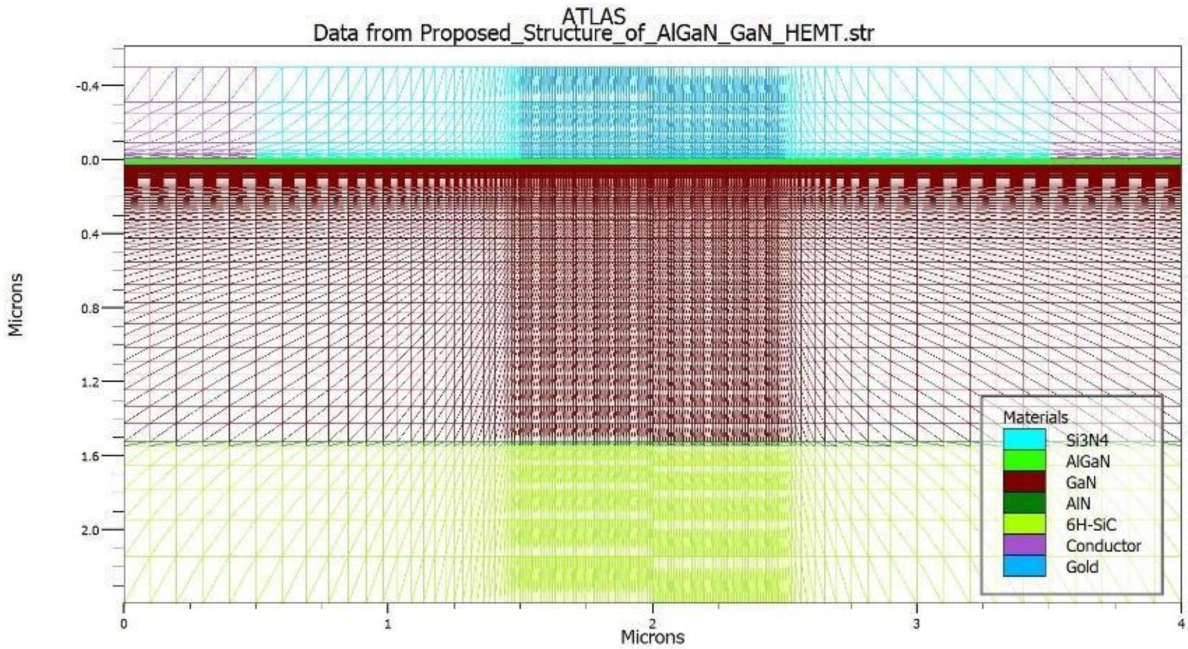

Fig-3.3: Mesh diagram of the proposed structure

We have done n-type doping in the AlGaN channel of $1x10^{18}cm^{-3}$ which facilitates the growth of 2DEG at the interface between AlGaN and GaN layers. The net absolute doping in the proposed structure is shown in Fig-3.4.

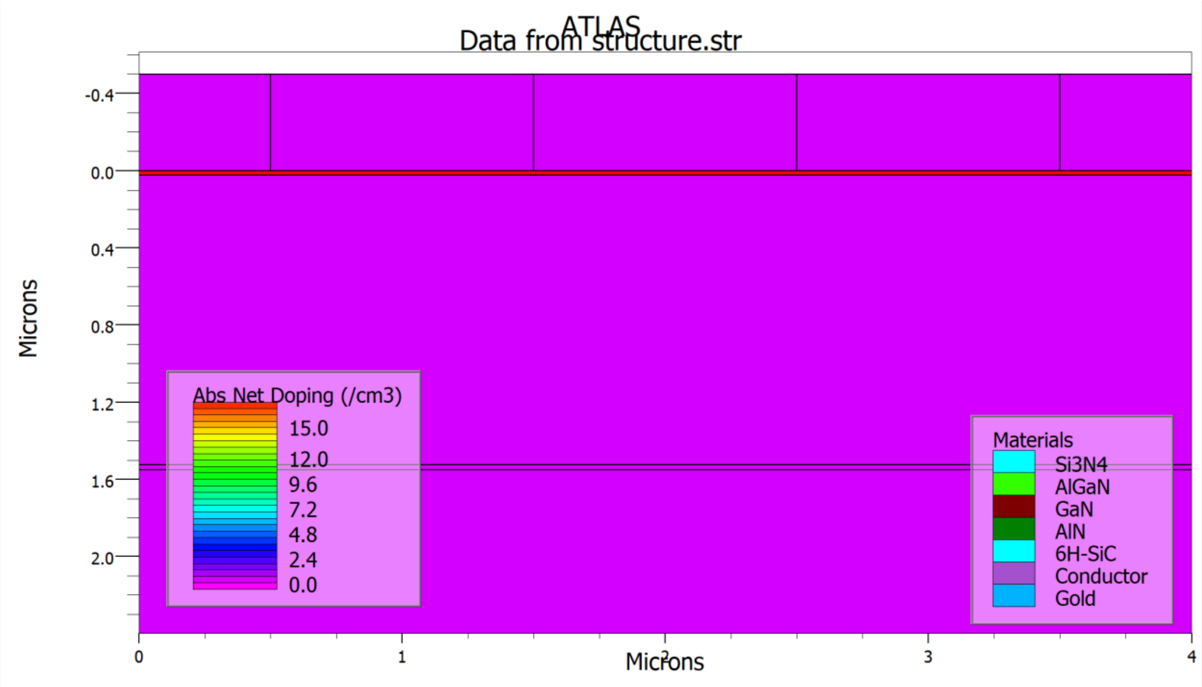

Fig-3.4: Net absolute doping in the structure

3.4 Conclusion

This chapter gave information about the software used for this simulation-based project- Silvaco TCAD. Also, we have shown proposed the HEMT structure used for this project. The mesh structure and the doping concentration have been shown to give an in-depth knowledge about the structure. Various analyses have been done on this HEMT structure, namely, the DC analysis, effects of structural variations and temperature variations on the device characteristics and RF analysis, and have been discussed in the subsequent chapters.

CHAPTER 4

DC ANALYSIS

4.1 Introduction

This chapter deals with the DC analysis of the AlGaN/GaN HEMT. We have run the DC simulation at 300K to obtain the transfer characteristics and output characteristics; and extracted the transconductance curve from the transfer characteristics curve for our proposed HEMT device (Fig-3.2).

The transfer characteristics relates drain current (I_D) response to the input gate-source driving voltage (V_{GS}). Since the gate terminal is electrically isolated from the remaining terminals (drain, source and bulk), the gate current is essentially zero, so that gate current is not part of the device characteristics. The output characteristics, also called as the drain characteristics, of the HEMT are drawn between the drain current (I_D) and the drain-to-source voltage (V_{DS}).

The transconductance is the ratio of the change in current at the output terminal (I_D) to the change in the voltage at the input terminal (V_{GS}) of the HEMT device.

4.2 Observations from the DC analysis of the proposed AlGaN/GaN HEMT device

The transfer characteristics and output characteristics of the device from the proposed structure of AlGaN/GaN HEMT on SiC substrate (as shown in Fig-3.2) are given in Fig-4.1 and Fig-4.2 respectively. The extracted transconductance curve is given in Fig-4.3; Fig-4.4 shows the plot of drain current (I_D) and transconductance w.r.t. gate voltage (V_{GS}).

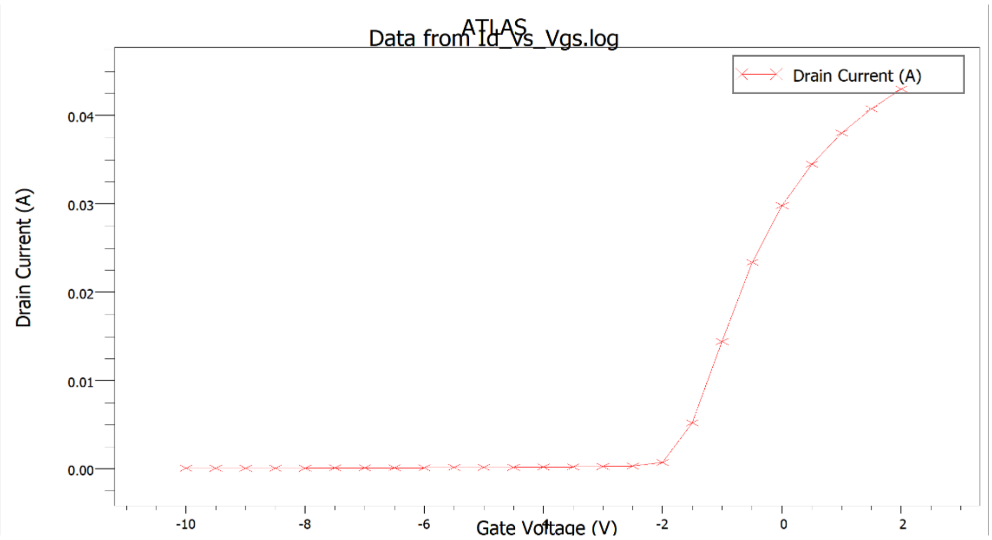

Fig-4.1: Transfer characteristics of AlGaN/GaN HEMT on SiC substrate

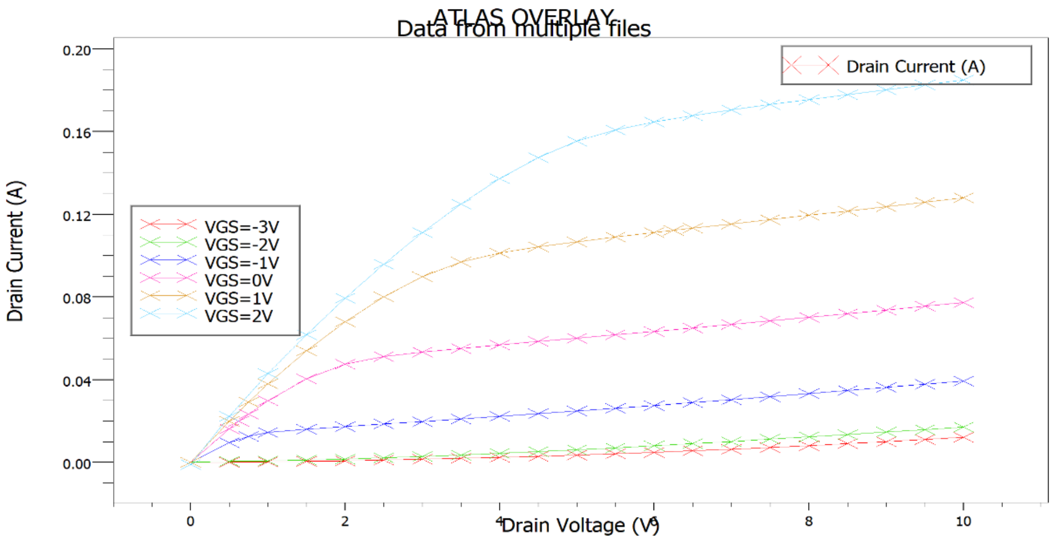

Fig-4.2: Output characteristics AlGaN/GaN HEMT on SiC substrate

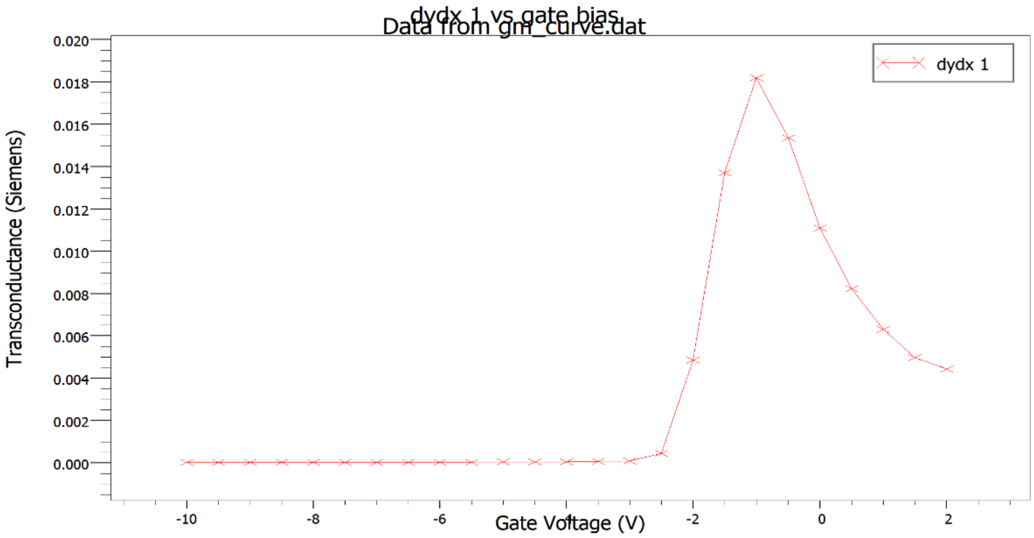

Fig-4.3: Transconductance curve of AlGaN/GaN HEMT on SiC substrate

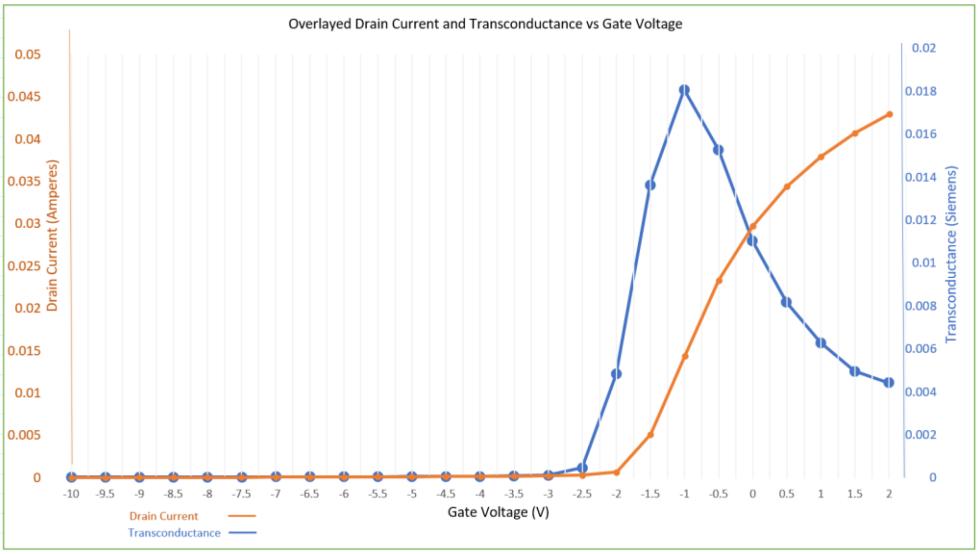

Fig-4.4: Transconductance and Drain current w.r.t. Gate Voltage of AlGaN/GaN HEMT

Due to the mismatch of energy bandgap of AlGaN and GaN, band bending occurs at the interface of the two materials. This gives rise to the formation of 2DEG at the channel. The bend bending is illustrated in Fig-4.5(a) and Fig-4.5(b).

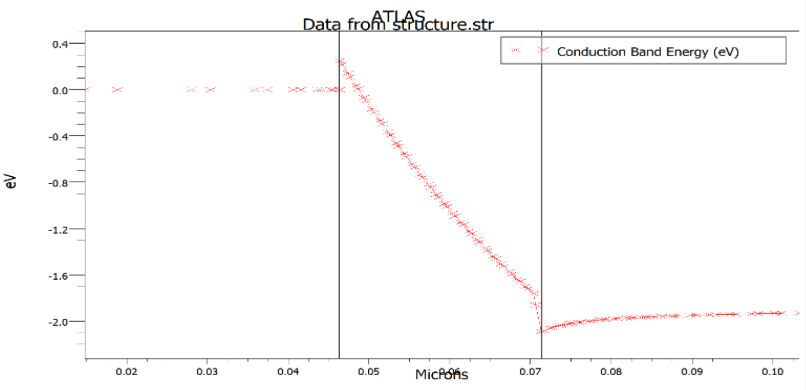

(a)

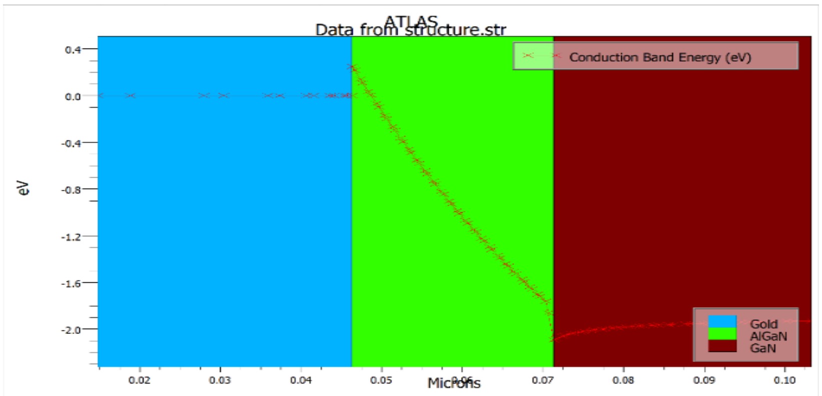

(b)

Fig-4.5 (a) and (b): Bending of the conduction band resulting in the formation of 2DEG

4.3 Conclusion

The results obtained from the above analyses and observations can be summarised as mentioned below.

We have extracted the threshold voltage (V_{th}) from the plot shown in Fig-4.1 (using the formula as given in [38] to extract x-intercept) and can conclude that the threshold voltage of the device is -2.28V, which is comparable with the values provided in [6], and is favourable for high power applications. Also, from Fig-4.7, we can conclude that the transconductance reaches peak value of 0.0182 Siemens (S) or 18.2 mS, which occurs slightly above the threshold voltage at V_{GS} = -1V. The n-type doping of $1\text{x}10^{18}$ done in the AlGaN channel (as shown in Fig-3.4) facilitates the growth of 2DEG. Fig-4.5(a) and Fig-4.5(b) show the bending of the conduction band which occurs when two materials with different energy bandgaps are placed on top of other. It is to note here that the AlGaN has a higher bandgap then GaN.

CHAPTER 5

STRUCTURAL VARIATION AND ITS EFFECTS

5.1 Introduction

To find the optimal design of the proposed structure, we have varied the various structural parameters like width of the AlGaN channel, mole fraction of the Aluminium in AlGaN, doping concentration of the channel and work function of the gate material. One parameter has been varied by keeping the others constant, and after running the DC simulations for each parameter, we have tried to find out the optimum values for each parameter which yield better results.

Using this approach, we have also studied how the output current, threshold voltage and transconductance varies with changes in the structural properties.

5.2 Variation of AlGaN width

We have varied the width of the AlGaN channel from 0.01-0.03μm, and have run the DC simulations. The variation of threshold voltage with respect to change in width of the AlGaN channel have been shown below:

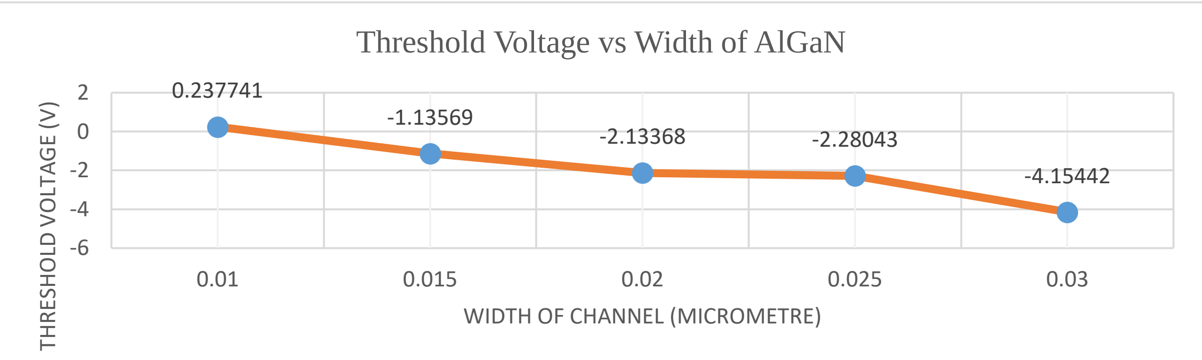

Fig-5.1: Plot showing the variation of threshold voltage (V_{th}) w.r.t. width of AlGaN

From the Fig-5.1, we observe that there is a negative shift of V_{th} with an increase in width of the AlGaN channel. For power applications, the threshold voltage is preferred to be in the range of -2 to -3V [6]. Hence, we have chosen 25nm (0.025μm) to be the width of the AlGaN channel which yields a threshold voltage of -2.28V.

5.3 Variation of doping concentration of AlGaN channel

We have varied the doping concentration of the AlGaN channel and run the simulations for the following concentrations: $1x10^{17}$, $1x10^{18}$, $2x10^{18}$, $3x10^{18}$, $4x10^{18}$, $5x10^{18}$ and $1x10^{19}$ (all units in cm^{-3}). The variation of threshold voltage, maximum drain current and peak transconductance, with respect to the change in the doping concentration of the AlGaN channel have been shown below:

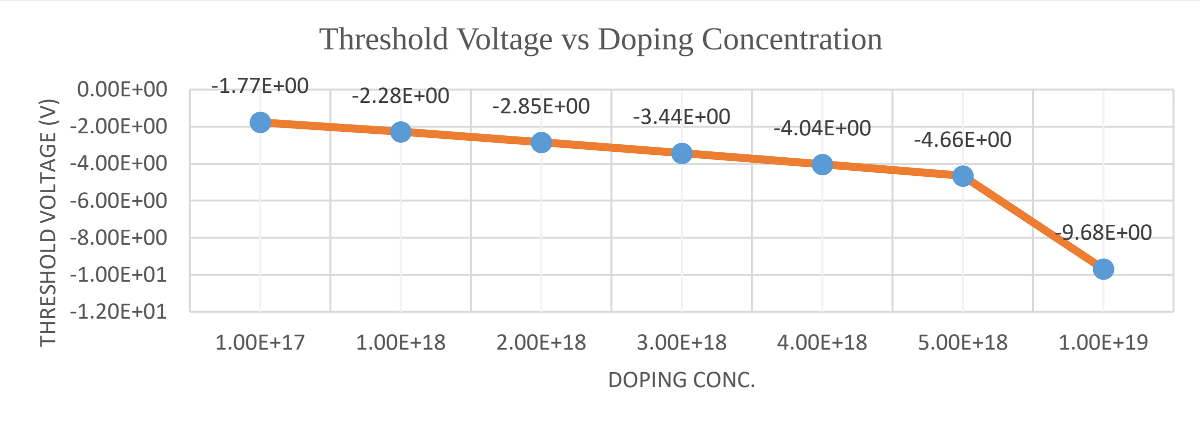

Fig-5.2: Plot showing the variation of threshold voltage (V_{th}) w.r.t. doping conc. of AlGaN

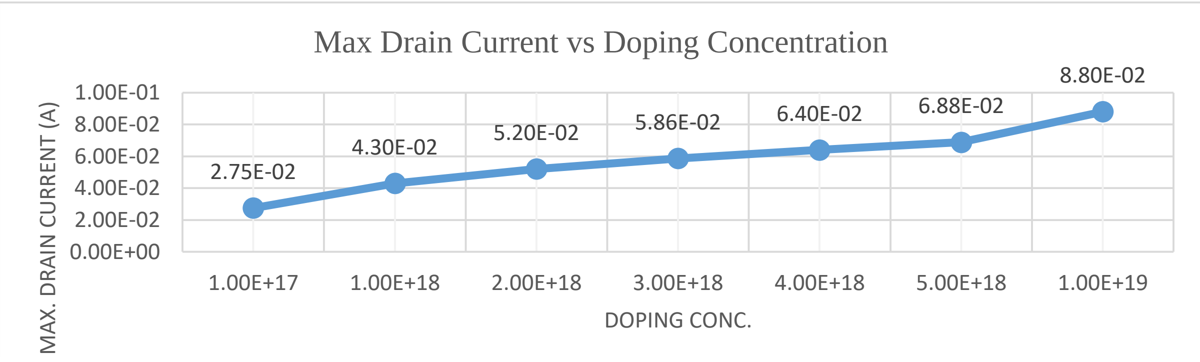

Fig-5.3: Plot showing the variation of maximum drain current (at V_{GS}=2V) w.r.t. doping conc. of AlGaN

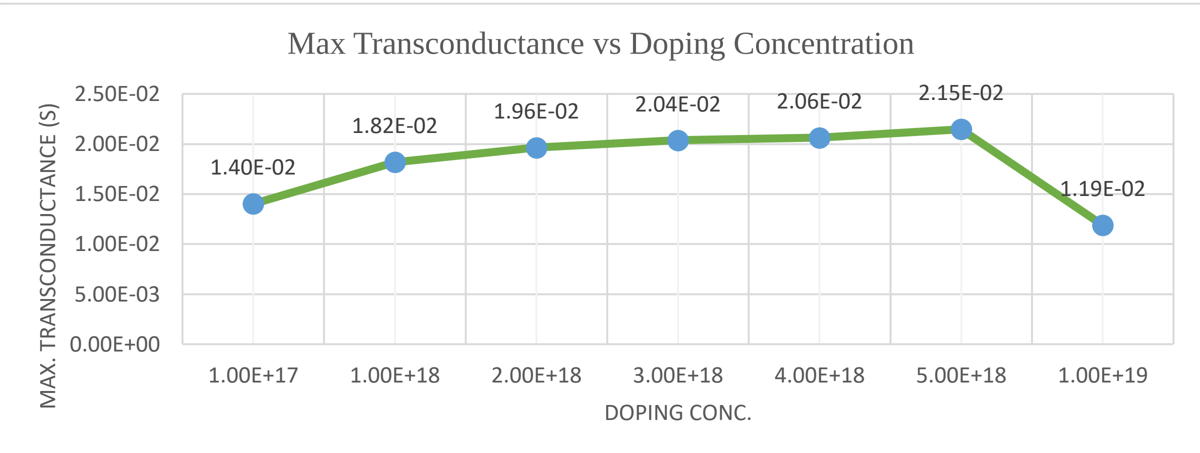

Fig-5.4: Plot showing the variation of peak transconductance (g_m) w.r.t. doping conc. of AlGaN

From the above figures (Fig-5.2, 5.3 and 5.4), it is evident that a doping concentration of $2x10^{18}cm^{-3}$ yields a threshold voltage lying between -2 and -3V, as well as a higher peak value of drain current (I_D = 52mA at V_{GS} = 2V) and transconductance (g_m = 19.6 mS at V_{GS} = -1V). But, as we will see in the subsequent chapters about the noise figure of the device during RF analysis, this doping concentration leads to a higher minimum noise figure (as shown in Fig-7.11) as compared to the noise figure by a doping concentration of $1x10^{18}$ cm^{-3} (as shown in Fig-7.10). So, to obtain a lower minimum noise figure, we have chosen the doping concentration to be $1x10^{18}$ cm^{-3} which yields a threshold voltage (V_{th}) of -2.28V, maximum drain current of 43mA (at V_{GS} = 2V) and peak transconductance (g_m) of 18.2 mS (at V_{GS} =-1V).

5.4 Variation of mole fraction of Aluminium in AlGaN channel

We have varied the mole fraction of Aluminium from 20% to 35% in the AlGaN channel, and run the DC simulations to obtain the optimum value of mole fraction of Aluminium which gives better results. Moreover, this also helps in understanding how mole fraction of Al in the channel affects the device characteristics.

The results obtained have been shown below:

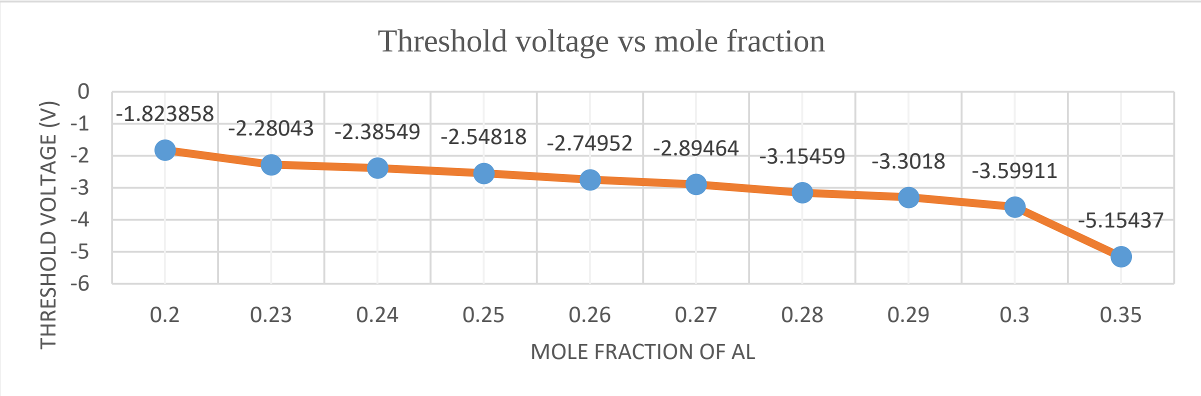

Fig-5.5: Plot showing the variation of threshold voltage (V_{th}) w.r.t. mole fraction of Al in AlGaN

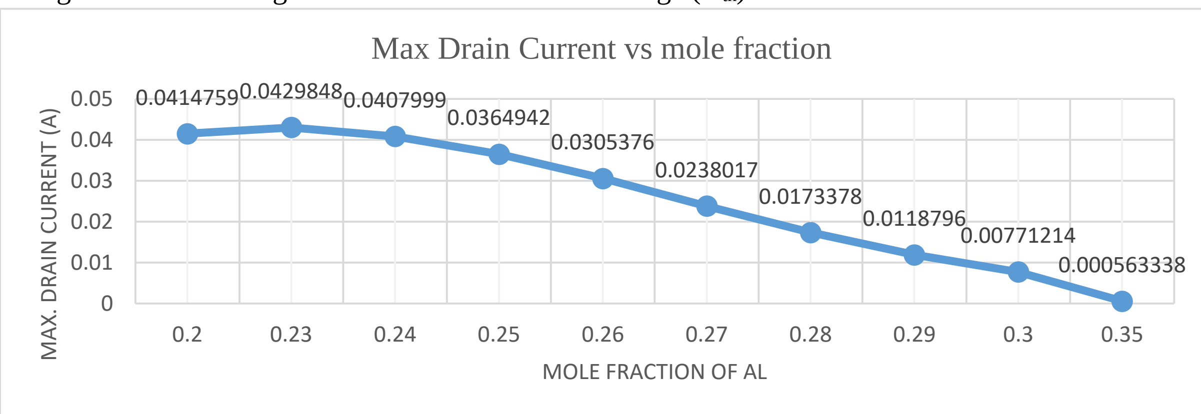

Fig-5.6: Plot showing the variation of maximum. drain current w.r.t. mole fraction of Al in AlGaN

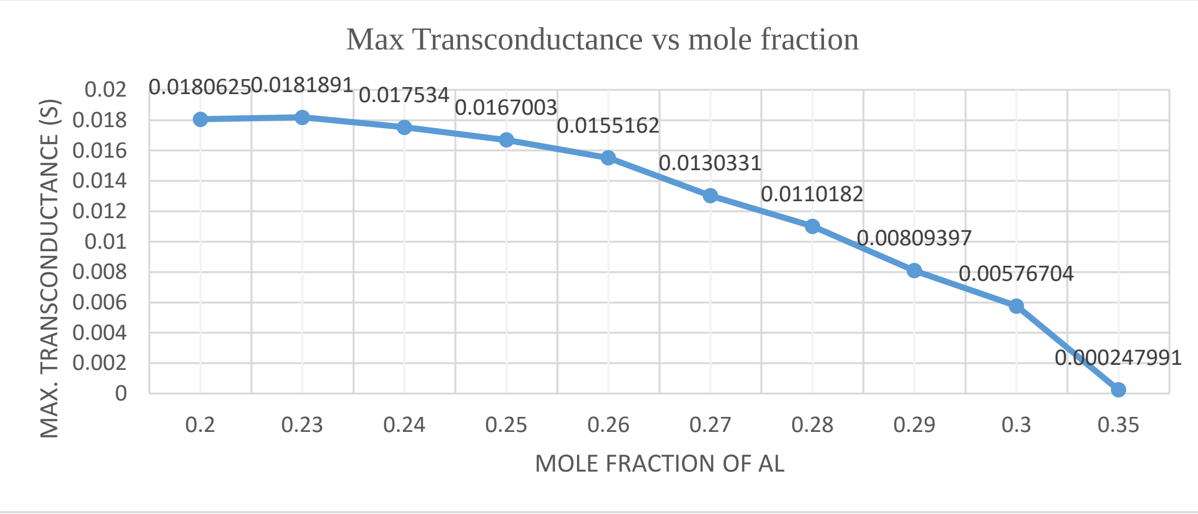

Fig-5.7: Plot showing the variation of max. transconductance w.r.t. mole fraction of Al in AlGaN

From the above figures (Fig-5.5, 5.6, 5.7), it is evident that at 23% of Al in the AlGaN channel, we obtain a threshold voltage (V_{th}) of -2.28V, and peak value of drain current (I_D) of 42.9mA (at V_{GS} = 2V) and peak transconductance (g_m) of 18.2 mS (at V_{GS} = -1V). Hence, we have chosen $Al_{0.23}GaN_{0.77}$ as the channel.

5.5 Variation in work function of gate material

The work function of the gate is determined by the choice of gate material used. We have used a variety of gate materials and studied the characteristics of the device. This study has helped us choose the appropriate gate material which yields the desired results for the device.

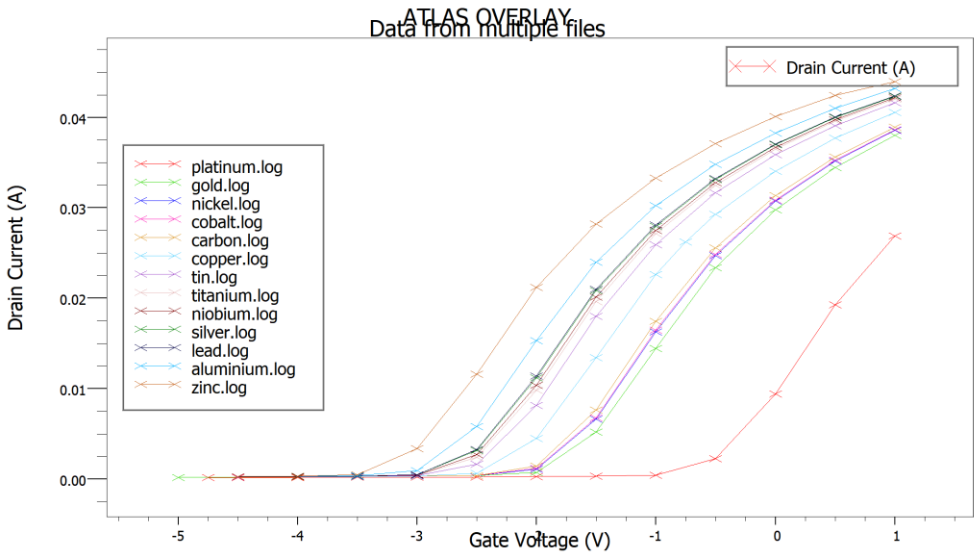

Fig-5.8: Combined transfer characteristics of the device using various gate materials

From Fig-5.8, we observe that, there is a shift in the threshold voltage with different gate materials having different work functions. This is further illustrated in the plots given below.

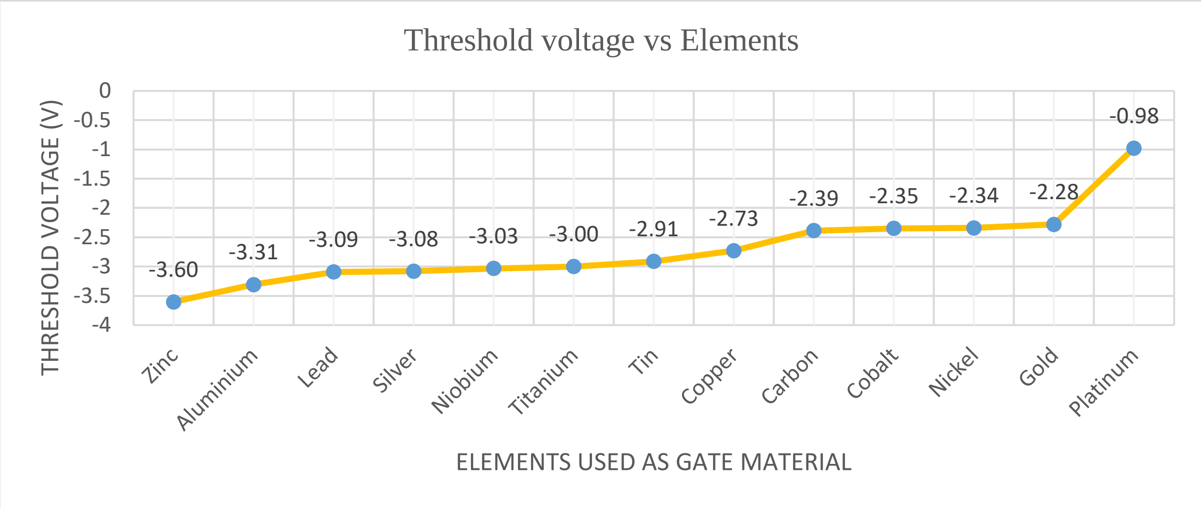

Fig-5.9: Plot showing the variation of threshold voltage w.r.t. different gate materials used

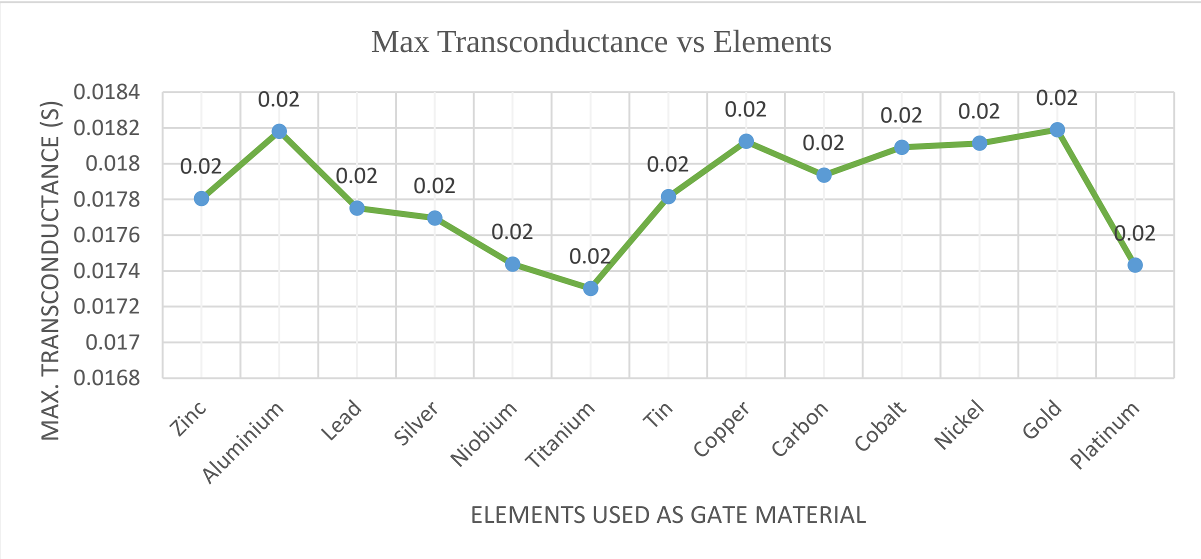

Fig-5.10: Plot showing the variation of max. transconductance w.r.t. different gate materials used

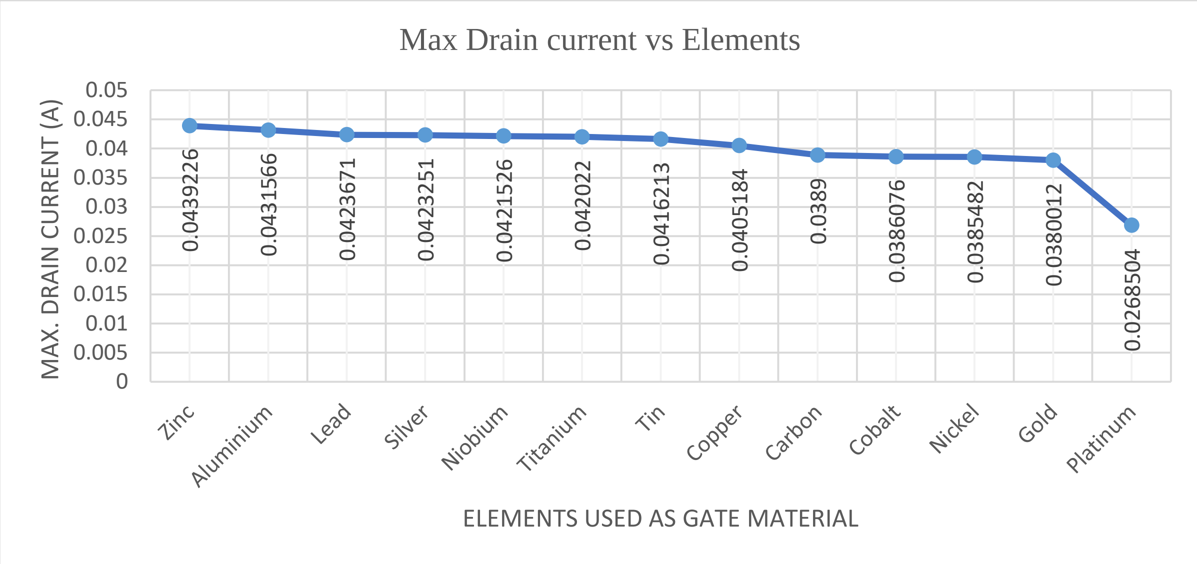

Fig-5.11: Plot showing the variation of max. drain current w.r.t. different gate materials used

With the combined results from plots in figures Fig-5.9, 5.10 and 5.11, we observe that we obtain a V_{th} = -2.28V, I_D = 40 mA (at V_{GS} = 2V), and g_m = 18.2 mS (at V_{GS} = -1V), when Gold (with work function of 5.1eV) is used as the gate material.

5.6 Conclusion

This chapter dealt with the variations of the structural parameters of the AlGaN/GaN HEMT and how they affect the device characteristics like threshold voltage, maximum drain current and peak transconductance. This has helped use choose the most optimum values for each parameter so that we obtain the best possible results.

CHAPTER 6
EFFECT OF TEMPERATURE VARIATION

6.1 Introduction

An essential component of the performance and dependability of AlGaN/GaN HEMTs is their temperature dependence. At low temperatures, the devices show enhanced electrical properties such low sheet resistance and high electron mobility. The 2DEG properties, including mobility and sheet carrier density, are maintained at very low temperatures, resulting in enhanced device performance.

While most high-power applications operate at room temperature, there are many specialized applications in fields like space, medicine, and energy that can leverage the advantages of low temperature operation around 0°C to improve efficiency, power density, and performance [39]. The unique material properties of AlGaN and GaN, including wide bandgap, high critical electric field, and high electron mobility, enable AlGaN/GaN HEMTs to operate at high power levels even at low temperatures around 0°C. This makes them attractive for a wide range of high power, high frequency applications in communications, radar, power electronics, and instrumentation [40]. Ongoing research is further improving their performance and reliability. This chapter deals with variation of temperature and its effects on the device characteristics, and from the results, we have obtained the operating temperature range of the proposed structure of the AlGaN/GaN HEMT device.

The operating temperature range refers to the range of temperatures within which a device or component can function properly without significant degradation or failure. In the context of AlGaN/GaN HEMTs, the operating temperature range is the range of temperatures at which the device can operate stably and maintain its desired performance characteristics.

6.2 Variation of temperature and its effects on the device characteristics

We have varied the temperature of the DC simulations from 250K to 500K, and obtained the device characteristics for each temperature, then studied the effect of variation of temperature on the threshold voltage, drain current and transconductance of the device. This study has also helped us determine the operating temperature of the device. The results of the study are shown in the following plots.

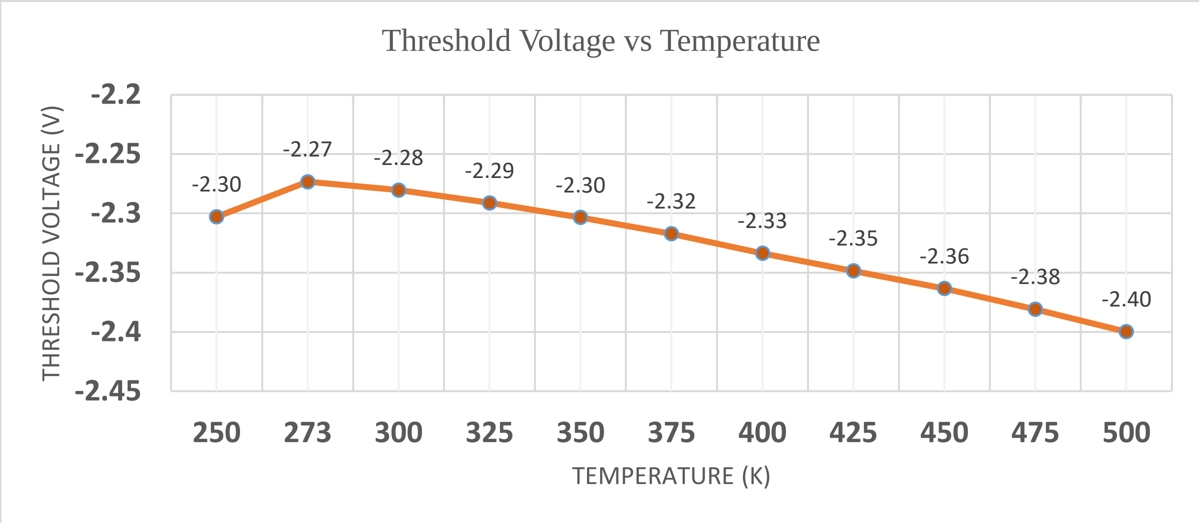

Fig-6.1: Plot showing the variation of threshold voltage w.r.t. temperature

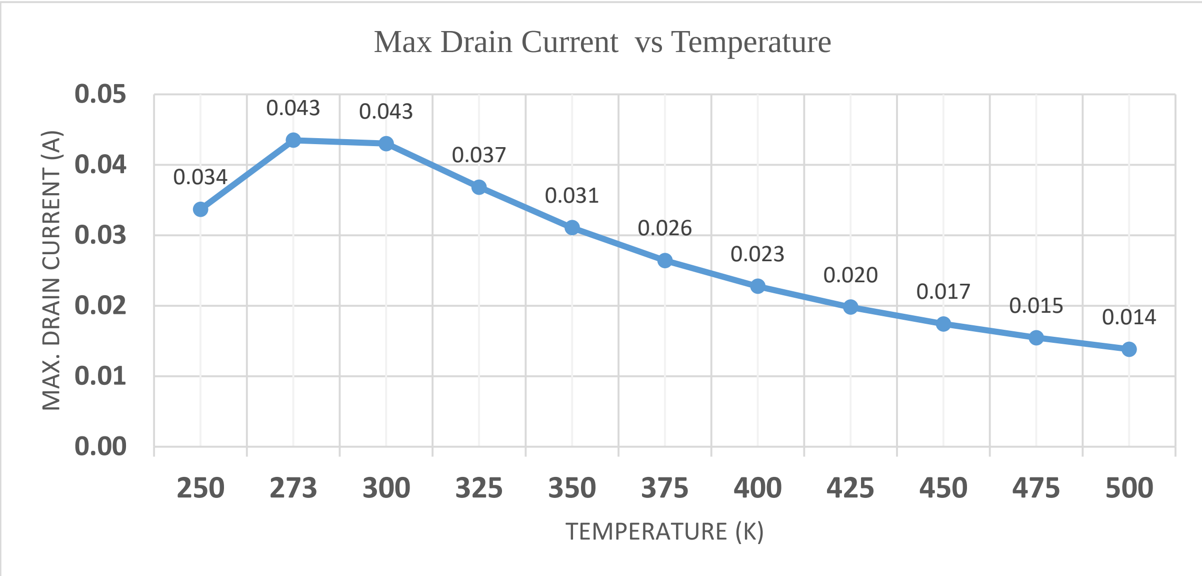

Fig-6.2: Plot showing the max. drain current w.r.t. temperature

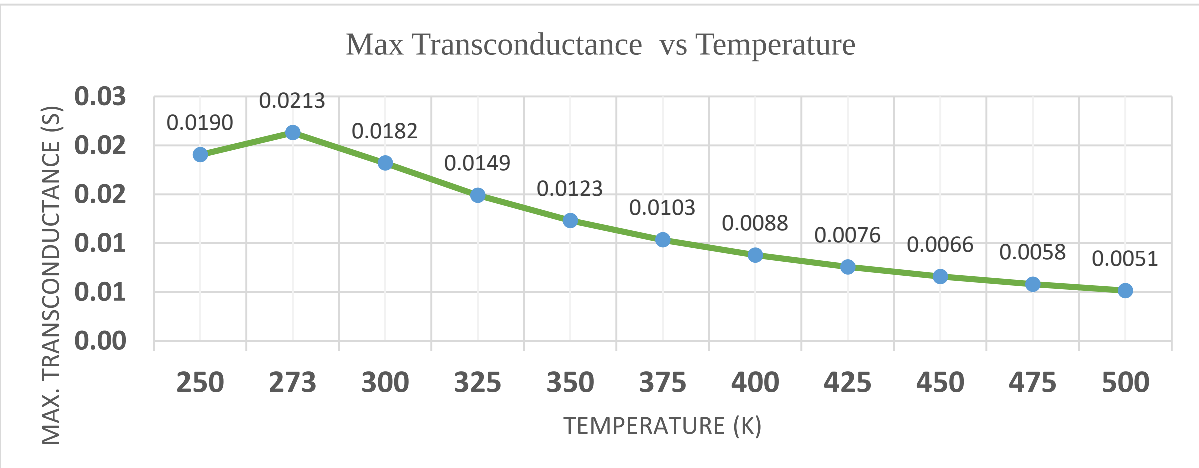

Fig-6.3: Plot showing the peak transconductance w.r.t. temperature

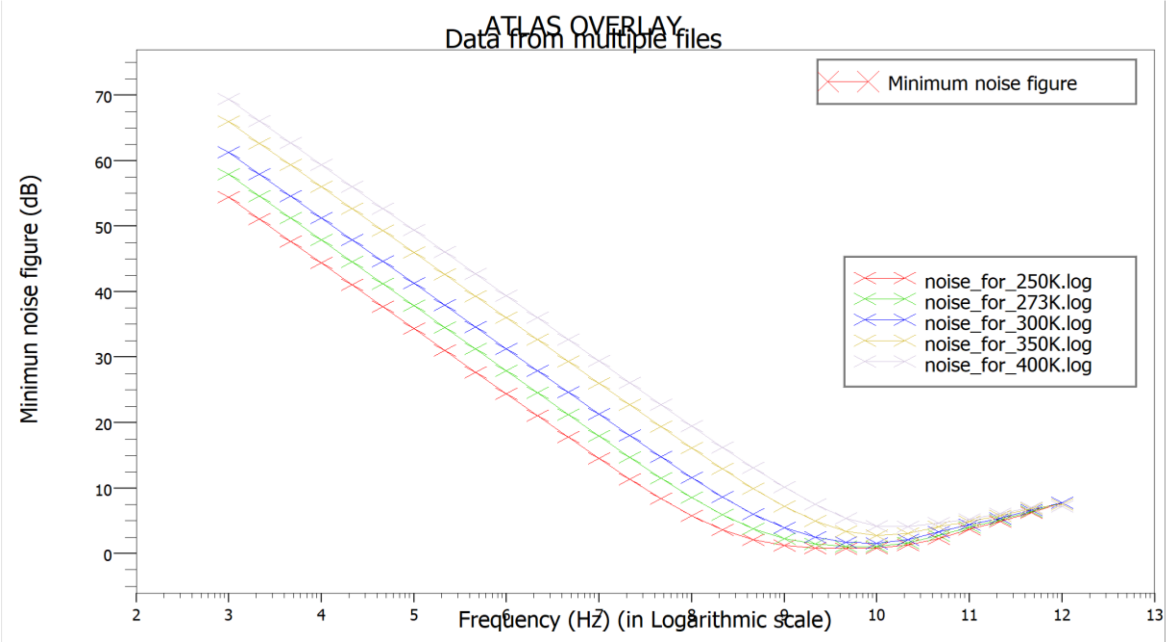

Fig-6.4: Plot showing the noise figure w.r.t. temperature

6.3 Inferences

- Fig-6.1 shows that with increase in temperature, the threshold voltage (V_{th}) becomes more negative. This is due to the increase in electron concentration [41].
- From Fig-6.2, we observe that the maximum value of drain current (I_D) (at V_{GS} = 2V) is 43mA in the temperature range of 273K-300K, and then decreases gradually with further increase of temperature up to 500K.
- From Fig-6.3, we observe that the peak value of transconductance (g_m) occurs at 21.3mS at 273K, and with increase of temperature, the transconductance value gradually decreases. This decrease of transconductance with increase of temperature is due to the temperature-dependence of mobility where mobility of 2DEG channel decreases with increasing temperature [45, 46]; temperature-induced defects [42], and thermal noise [42].
- From Fig-6.4, we observe that the noise figure increases with increase in temperature which indicates that the device performance degrades with increase in temperature. This is due to addition of thermal noise [42].
- With the above results, we can conclude that the device has an operating temperature range of about 273-300K

CHAPTER 7
RF ANALYSIS

7.1 Introduction

The radio frequency (RF) performance of HEMT (High Electron Mobility Transistor) transistors is assessed, with an emphasis on the transistors' capacity to function at higher frequencies with greater power density. Understanding the operation of HEMTs in high-frequency applications, like sensor components, space technologies, and radar communications, depends on this approach. The capacity of HEMTs to handle high-frequency signals well is indicated by RF analysis, which makes them useful for a variety of applications needing high-speed and high-power operation. The process entails evaluating variables such as gain, power output, efficiency, and linearity to guarantee peak performance in radio frequency circuits and systems.

In this chapter, we have performed the RF analysis on the proposed structure of the AlGaN/GaN HEMT device and have found out the capacitances (C_{GS} and C_{GD}), cut-off frequency of the device and the minimum noise figure (NF_{min}) of the device.

C_{GS} and C_{GD} are two significant capacitances of a High Electron Mobility Transistor (HEMT) that are essential to the transistor's functioning. By varying the bias voltage, these capacitances are used to represent changes in the depletion region.

- C_{GS} (Gate-Source Capacitance): This capacitance represents the capacitance between the gate and the source of the HEMT. It is typically a function of the gate-source voltage (V_{GS}) and is responsible for the charge storage and depletion of the channel region. C_{GS} is an important parameter in determining the transistor's input impedance and its ability to handle high-frequency signals [44].
- C_{GD} (Gate-Drain Capacitance): This capacitance represents the capacitance between the gate and the drain of the HEMT. It is also a function of the gate-source voltage (V_{GS}) and is responsible for the charge storage and depletion of the channel region. C_{GD} is an important parameter in determining the transistor's output impedance and its ability to handle high-frequency signals [44].

Understanding the behaviour of HEMTs in RF circuits and systems, where high-frequency signals are present, requires an understanding of these capacitances. The transistor's gain, power output, efficiency, and linearity are determined by them, which makes them essential for a variety of applications that need high-speed and high-power operation.

An AlGaN-GaN HEMT device's cut-off frequency is a crucial factor in determining how well it performs at high frequencies. It is described as the frequency at which the device's gain drops to unity (or 0 dB), or the point at which the output power and input power of the device are equal [45].

The cut-off frequency is significant because it reflects the highest frequency at which the device can run without significantly losing gain. It is an indicator of how well the device can amplify high-frequency signals. Higher cut-off frequencies allow a device to operate at higher frequencies without experiencing appreciable performance deterioration, which makes them appropriate for high-frequency systems like millimetre-wave and microwave systems [48, 49]. In general, the cutoff frequency is a crucial factor for determining HEMTs' high-frequency performance and is used to establish which applications are best suited for them.

To obtain the cut-off frequency (f_T), we follow the following steps:

1. Obtain the transconductance (g_m) for various gate voltages from DC analysis.
2. Apply a small signal AC frequency to the gate terminal and perform the DC sweep again.
3. Obtain the Gate-to-Source Capacitance (C_{GS}) and Gate-to-Drain Capacitance (C_{GD}).
4. Apply the formula as shown to calculate the cut-off frequency (f_T) [47]:

$$f_T = \frac{g_m}{2\pi(C_{GS} + C_{GD})}$$

The minimum noise figure (NF_{min}) is a critical parameter in the context of HEMTs, particularly for low-noise applications like receivers [48]. It represents the lowest achievable noise figure of the device under optimum source impedance matching conditions. The ratio of the signal-to-noise ratio at the device's input to the signal-to-noise ratio at its output is known as the noise figure (NF). For low-noise amplifiers, a lower noise number is preferable since it denotes improved noise performance. Achieving a low minimum noise figure is essential for low-noise HEMT performance. Device parameters including the gate length, transconductance, and gate-source capacitance must be optimized.

7.2 Capacitances obtained after performing RF analysis and calculation of Cut-off frequency

From the DC analysis as shown in Chapter-4, we have obtained the transconductance (g_m) to be 0.0182 S or 18.2 mS.

We have performed the RF analysis by applying an AC signal with frequency of 300KHz, 1MHz, 10GHz and 40GHz; and obtained the C_{GS} and C_{GD} for each case. For each set of C_{GS} and C_{GD}, we have calculated the cut-off frequency (f_T) using the formula as shown in the previous section, for the corresponding applied frequency.

The results are shown as follows:

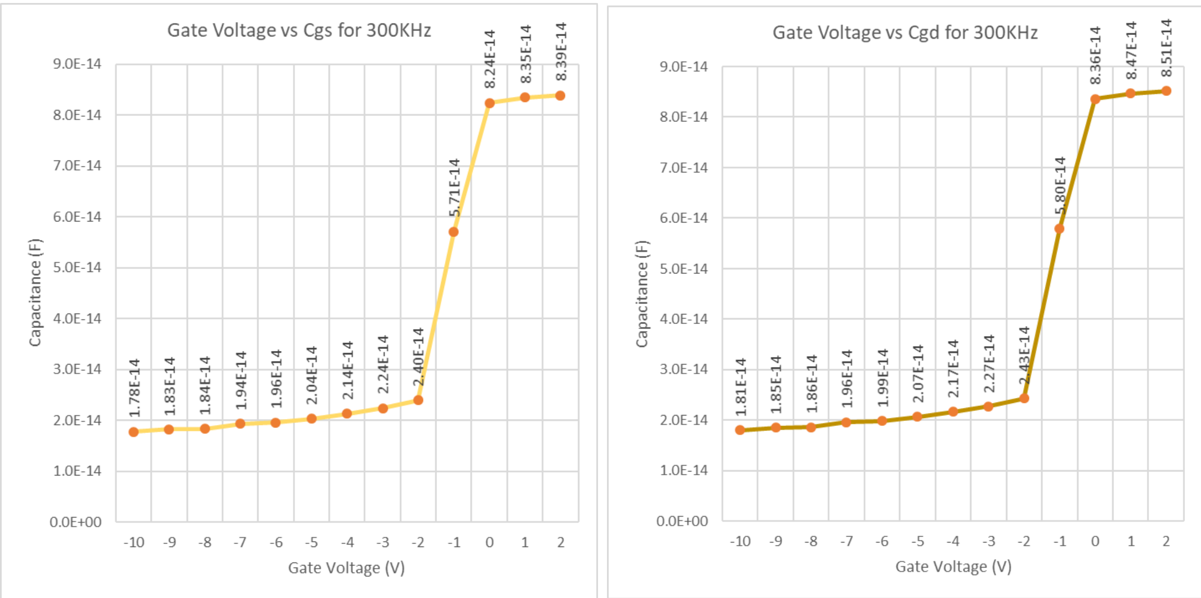

Fig-7.1: Plots depicting the C_{GS} and C_{GD} obtained for input signal of 300 KHz

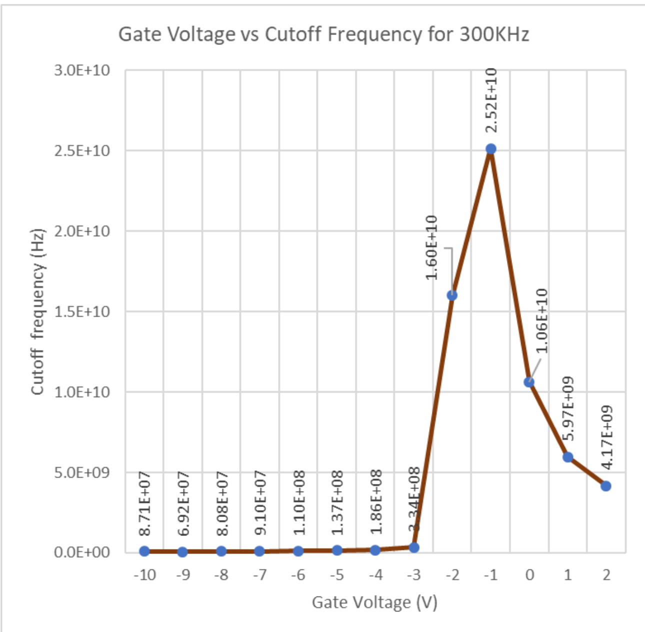

Fig-7.2: Plot depicting cut-off frequency obtained for input signal of 300 KHz

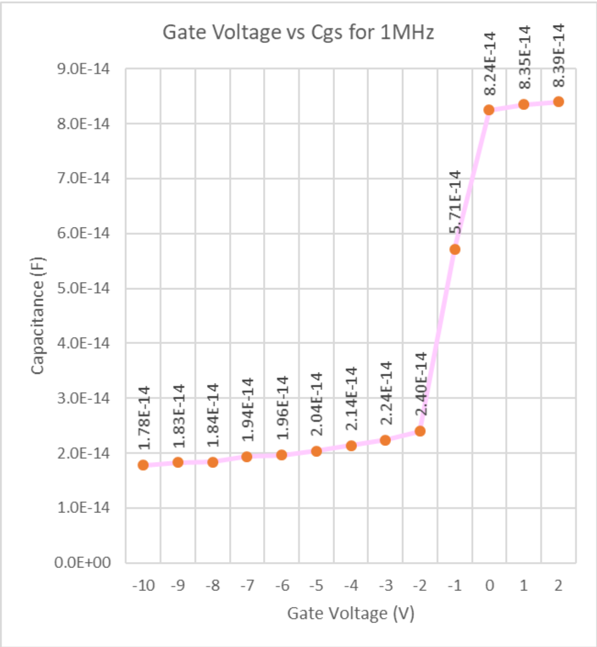

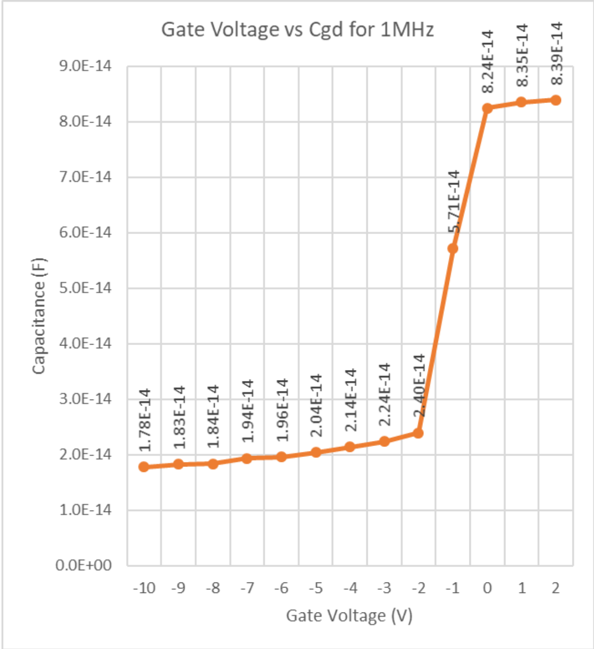

Fig-7.3: Plots depicting the C_{GS} and C_{GD} obtained for input signal of 1 MHz

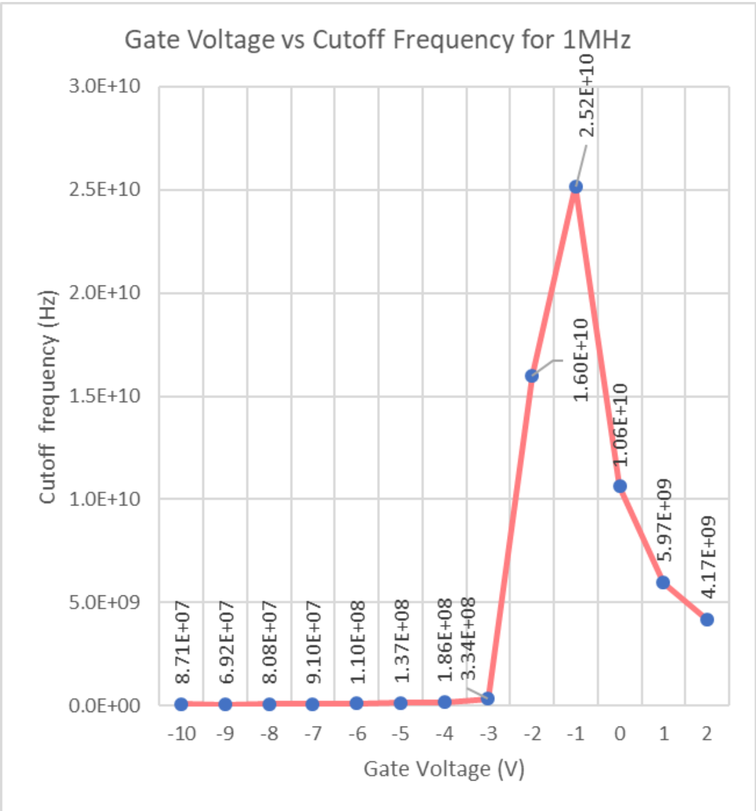

Fig-7.4: Plot depicting cut-off frequency obtained for input signal of 1 MHz

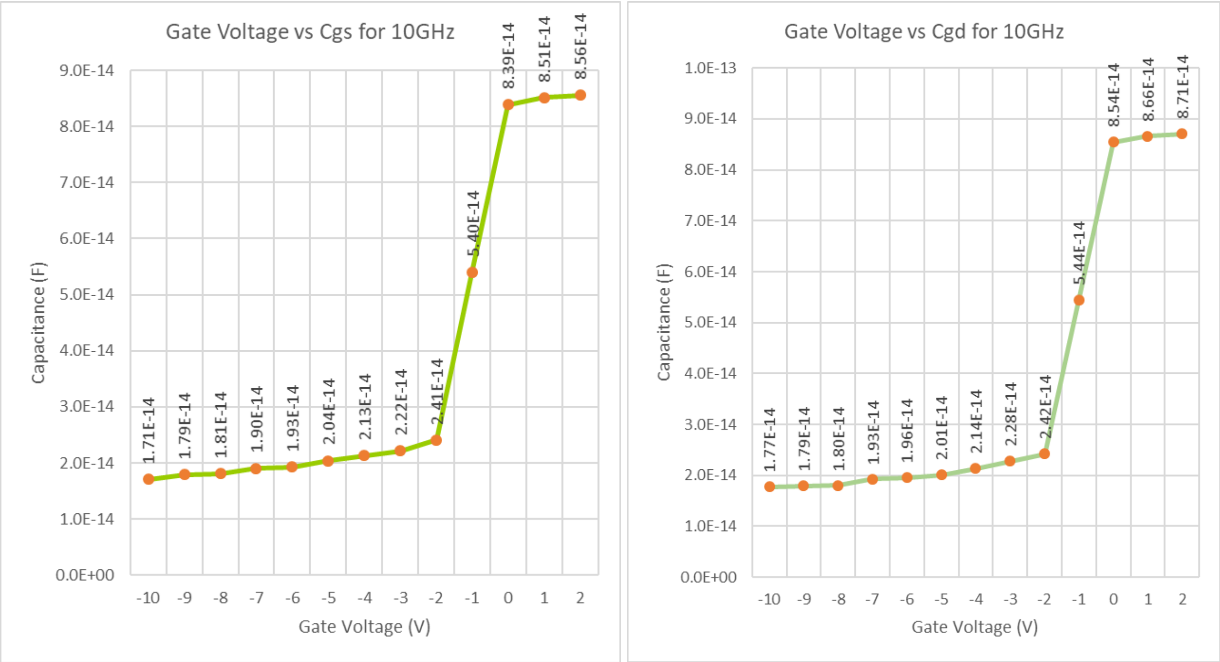

Fig-7.5: Plots depicting the C_{GS} and C_{GD} obtained for input signal of 10 GHz

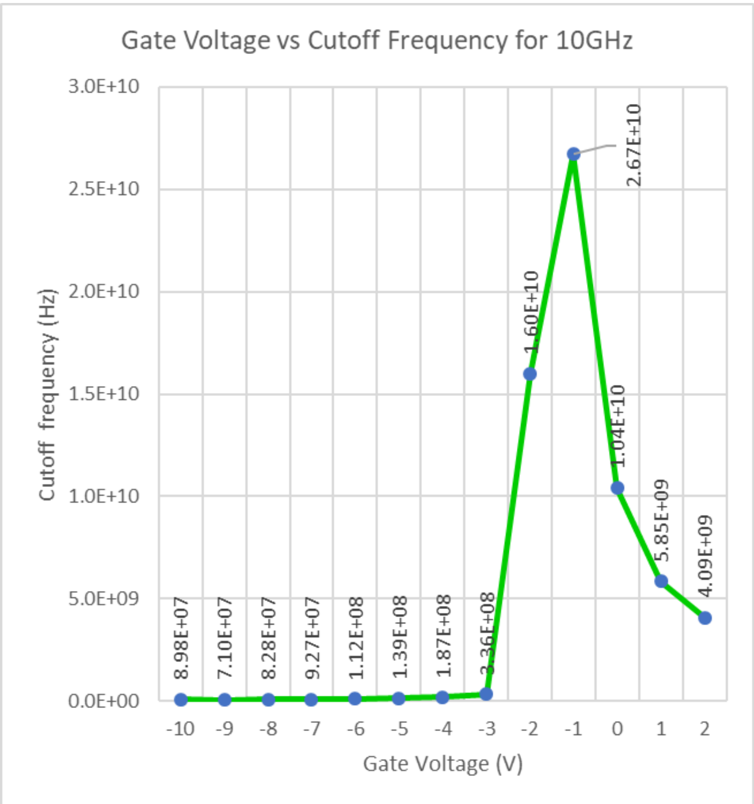

Fig-7.6: Plot depicting cut-off frequency obtained for input signal of 10 GHz

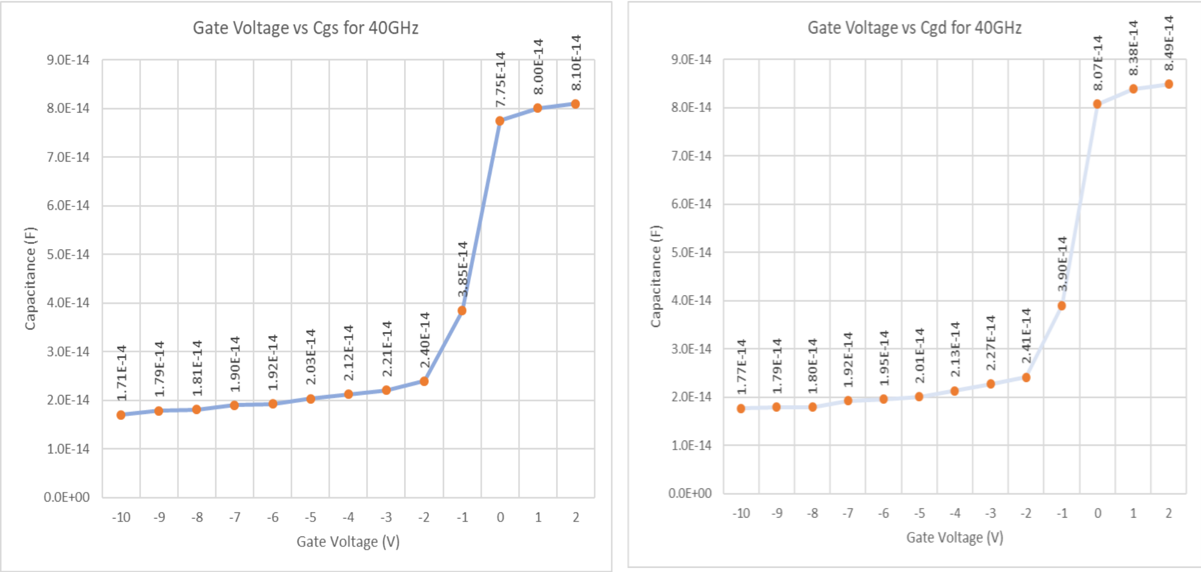

Fig-7.7: Plots depicting the C_{GS} and C_{GD} obtained for input signal of 40GHz

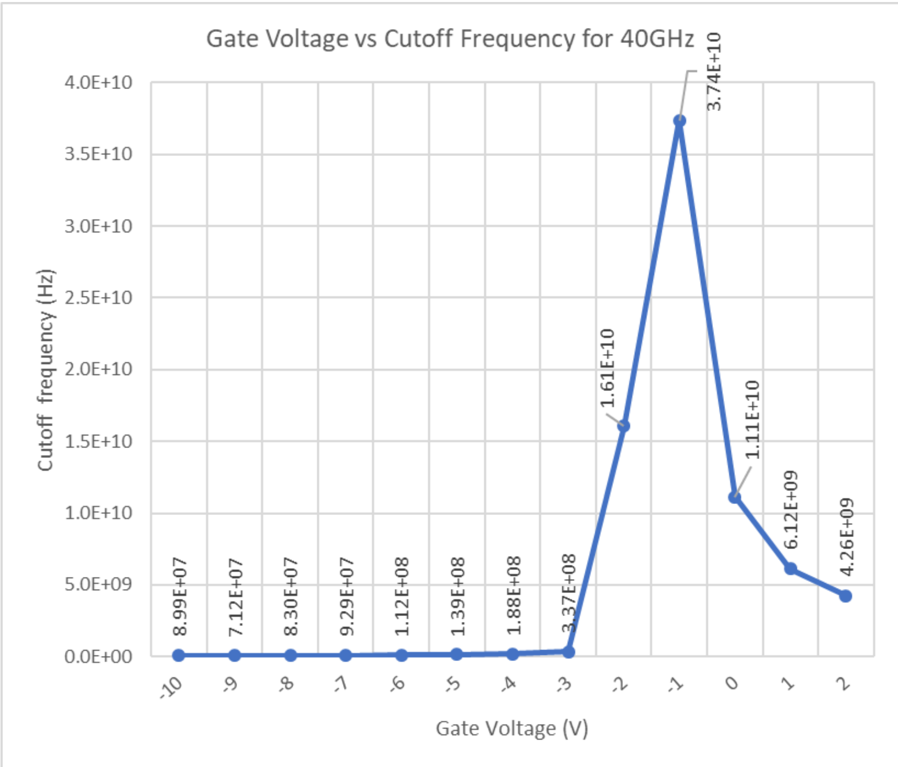

Fig-7.8: Plot depicting cut-off frequency obtained for input signal of 40 GHz

From the above plots, we infer the following:

- f_T = 25.2GHz at input signal of 300 KHz (Fig-7.2)
- f_T = 25.2GHz at input signal of 1 MHz (Fig-7.4)
- f_T = 26.7GHz at input signal of 10 GHz (Fig-7.6)
- f_T = 37.4GHz at input signal of 40 GHz (Fig-7.8)

Taking the average of the above cut-off frequencies, we can obtain the overall cut-off frequency of the device to be 28.625GHz. This lies in the Ka band of the radio spectrum (27-40 GHz), which is mainly used for RADAR and satellite communications [48].

7.3 Determination of the Minimum Noise Figure (NF_{min})

An important consideration in RF analysis is the noise figure of HEMTs (High Electron Mobility Transistors), especially when designing RF amplifiers and receivers. A HEMT's noise figure is a measurement of the extra noise the transistor itself introduces, which can lower the system's signal-to-noise ratio (SNR).

At high frequencies, the principal source of noise added by the transistor is related to power dissipation in the device resistances. At lower frequencies, generation/recombination processes become dominant. The minimum noise figure (NF_{min}) of an AlGaN/GaN HEMT decreases as the frequency increases from 2 GHz to 40 GHz, as shown in [49].

In our analysis, we have varied the input frequency from KHz (10^3 Hz) to THz (10^{12} Hz) range to study about the minimum noise figure of the device. The results have been shown below.

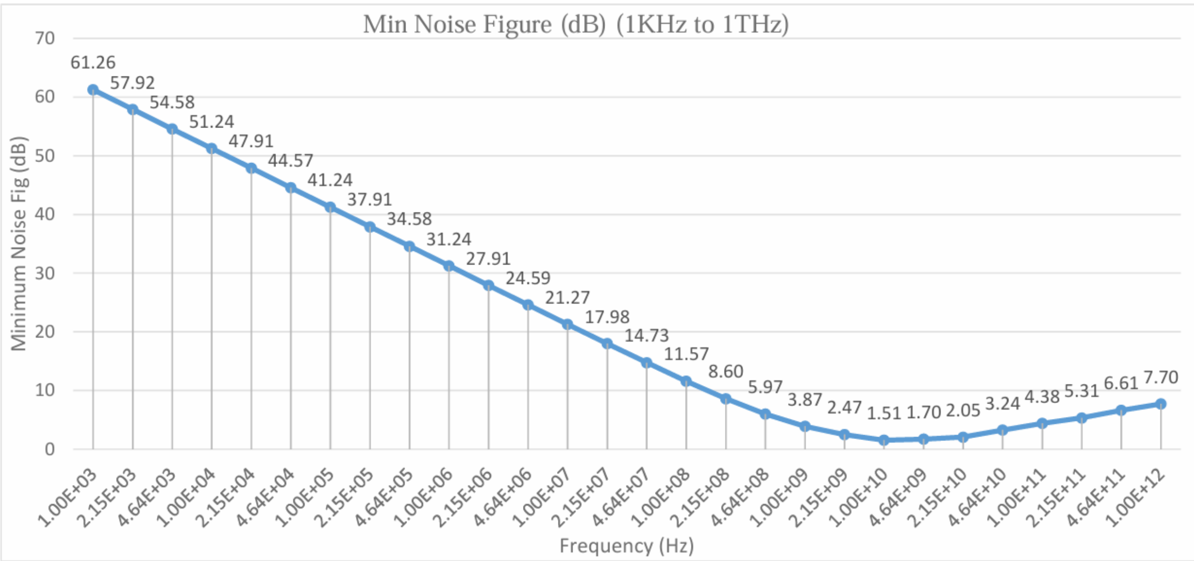

Fig-7.9: Plot for variation of NF_{min} w.r.t. frequency at the input

To get a proper insight into the NF_{min} at the operating frequency range (with our device having unity gain cut-off frequency (f_T = 28.625 GHz), we have plotted the NF_{min} by varying the frequency from 10GHz to 50GHz, covering the Ku band (12-18 GHz), the K band (18-26.5 GHz) and Ka band (26.5-40 GHz), and compared the results with [48].

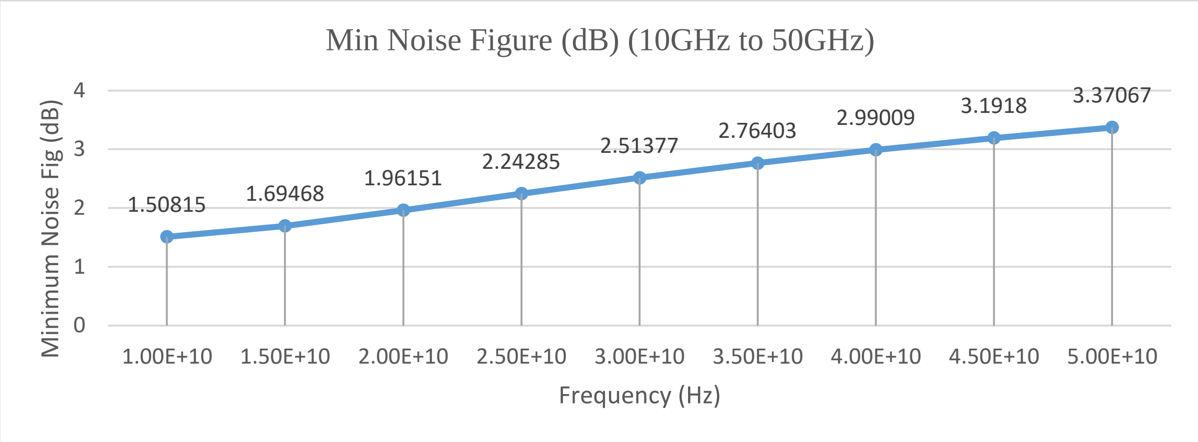

Fig-7.10: Plot for variation of NF_{min} w.r.t. frequency from 10-50 GHz

The NF_{min} at 10 GHz is 1.51 dB and that at 40 GHz is 2.99 dB, which is comparable with the results obtained in [48], which are good for low noise applications.

The NF_{min} in Fig-7.9 and 7.10 is plotted for a doping concentration of $1 \times 10^{18} cm^{-3}$ in the AlGaN channel. However, the value of NF_{min} increases with a higher doping concentration of $2 \times 10^{18} cm^{-3}$ (~5.27dB at 10GHz) as shown in the Fig-7.11, and a higher value of NF_{min} may lead to the device to perform poorly in low noise applications. Hence, we have chosen the doping concentration of the AlGaN channel to be $1 \times 10^{18} cm^{-3}$.

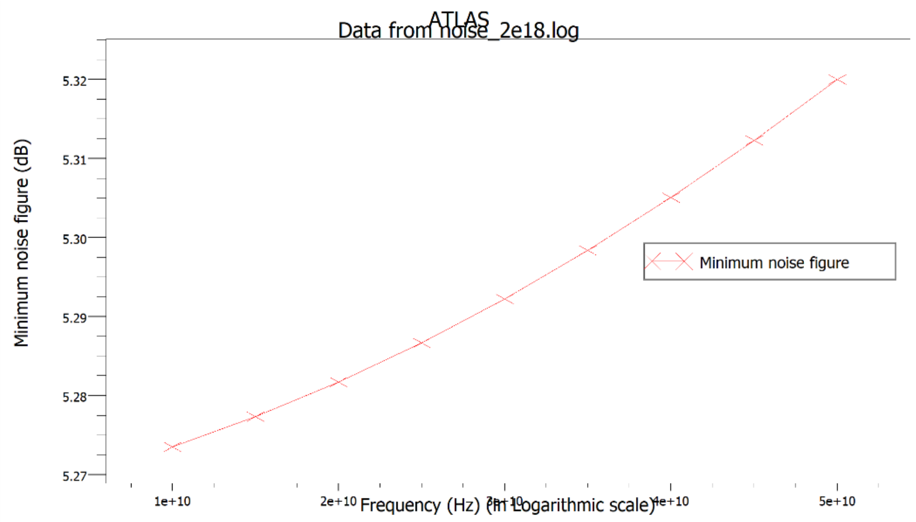

Fig-7.11: Plot for variation of NF_{min} w.r.t. frequency from 10-50 GHz for doping conc. of AlGaN channel to be $2 \times 10^{18} cm^{-3}$

It is to note that, this noise figure can be further improved by decreasing the gate length, with reference to [48].

CHAPTER 8

CONCLUSION AND FUTURE SCOPE OF WORK

8.1 Brief summary of the work

This thesis dealt with the design of AlGaN/GaN HEMT for high frequency and low noise applications using Silvaco TCAD. The proposed structure has been designed taking into account various earlier works, with parameters so chosen, that yields the best possible results. The device parameters of the structure have been shown in the table below.

Table-8.1: Device specifications of AlGaN/GaN HEMT

Material	**Thickness (in nm)**
$Al_{0.23}Ga_{0.77}N$	25
GaN	1500
AlN nucleation layer	25
SiC substrate	850
Gate length (Gate material = Gold with work function 5.1eV)	1000

Doping concentration of the AlGaN channel is $1x10^{18}cm^{-3.}$

After designing the HEMT structure, we have done the DC analysis of the structure, in which we have obtained the transfer characteristics and output characteristics at 300K. From these two plots, we have extracted the threshold voltage (V_{th}) and peak transconductance (g_m) of the device. Then, we have done an analysis on how the DC characteristics vary when the structural parameters like the width of AlGaN channel, the doping concentration of AlGaN channel, the mole fraction of Al in AlGaN channel and the work function of gate material, are varied. Further, we have also done a study on how the DC characteristics vary with a change in temperature. Then, we moved on to the RF analysis of the device, where we have found the gate capacitances, C_{GD} and C_{GS}, and calculated the cut-off frequency of the device. We have also found the minimum noise figure (NF_{min}) of the device which shows the amount of noise added to the output by the device itself.

8.2 Results obtained

- DC analysis:
    - Threshold voltage (V_{th}) = -2.28V
    - Peak transconductance (g_m) = 18.2mS, at V_{GS} = -1V
    - Drain current (I_D) = 43mA, at V_{GS} = 2V and V_{DS} = 1V
- Operating Temperature Range: 273-300K
- RF analysis:
    - Unity gain cut-off frequency (f_T) = 28.625GHz
    - Operating frequency range: Ka band of radio spectrum (26.5-40GHz)
    - Minimum noise figure (NF_{min}) = 1.51dB at 10GHz and 2.99dB at 40GHz

8.3 Fields of application

Based on the results obtained as shown in the previous section, we can conclude that the proposed structure of AlGaN/GaN HEMT can be used for high speed but low noise applications, such in low noise amplifiers in the RADAR and satellite communications [48] because of their high electron mobility and low noise figures. A Low-Noise Amplifier (LNA) is an electronic component specifically designed to amplify weak signals while minimizing the introduction of noise.

AlGaN/GaN HEMTs show promise in high-frequency power converters, particularly for applications like envelope tracking in radio frequency (RF) transmitters. Here, their ability to handle high frequencies and fast switching can be advantageous. Due to their excellent performance in Low-Noise Amplifiers (LNAs), AlGaN/GaN HEMTs can be integrated into power electronics systems alongside LNAs. This combined approach can offer benefits like improved overall noise figure and signal integrity in applications like radar or satellite communication systems.

8.4 Scopes of improvement

By optimizing the structural design, like reducing the gate length, and making further changes to the heterostructure layers, the transconductance value can be further increased to get comparable values as in [50], and to further reduce the minimum noise figure at higher frequencies by reducing the gate length [50].

REFERENCES

[1] Heterostructure and Quantum Well Physics, "Heterostructures and Quantum Devices", vol.24, Publisher -Elsevier, ISSN = 0736-7031

[2] P. A. Lee, N. Nagaosa, and X.-G. Wen, 'Doping a Mott insulator: Physics of high temperature superconductivity', Rev. Mod. Phys., vol. 78, pp. 17–85, Jan. 2006.

[3] Dingle, Raymond et al, "Electron mobilities in modulation-doped semiconductor heterojunction superlattices", Applied Physics Letters 33, 665-66, 1978

[4] Gossard, A.C. "Modulation Doping of Semiconductor Heterostructures." SpringerLink, Springer Netherlands, 1 Jan. 1985

[5] Das, Santanu. (2020). 2D Nanoscale Heterostructured Materials Synthesis, Properties, and Applications 1st Edition ISBN: 9780128176795.

[6] Nirmal, D., and J. Ajayan. "Handbook for III-V High Electron Mobility Transistor Technologies: D." Taylor & Francis, Taylor & Francis, 31 May 2019

[7] Hemaja, V., and D. K. Panda. "A Comprehensive Review on High Electron Mobility Transistor (HEMT) Based Biosensors: Recent Advances and Future Prospects and Its Comparison with Si-Based Biosensor - Silicon." SpringerLink, Springer Netherlands, 19 Feb. 2021

[8] H. L. Störmer, W.-T. Tsang, "Two-dimensional hole gas at a semiconductor heterojunction interface", Appl. Phys. Lett. 15 April, 36 (8): 685–687, 1980

[9] Mimura, Takashi et al, “A New Field-Effect Transistor with Selectively Doped GaAs/n-AlxGa1-xAs Heterojunctions”, Japanese Journal of Applied Physics 19, 1980

[10] Chen, C.Y. & Cho, A.Y. & Cheng, Kuei-Yueh & Pearsall, Thomas & O'Connor, P. & Garbinski, P.A, “Depletion Mode Modulation Doped Al//0//. //4//8In//0//. //5//2As-Ga//0//.//4//7In//0//. //5//3As Heterojunction Field Effect Transistors”, Electron device letters. 152-155. 1982

[11] Mohamed Aniss Mebarki, Ragnar Ferrand-Drake Del Castillo, Alexey Pavolotsky, Denis Meledin, Erik Sundin, Mattias Thorsell, Niklas Rorsman, Victor Belitsky and Vincent Desmaris, "GaN High-Electron-Mobility Transistors with Superconducting Nb Gates for Low-Noise Cryogenic Applications". Physica Status Solidi (a) applications and materials science, Volume 220, Issue 8, 2022.

[12] N. Keshmiri, D. Wang, B. Agrawal, R. Hou and A. Emadi, "Current Status and Future Trends of GaN HEMTs in Electrified Transportation," in IEEE Access, vol. 8, pp. 70553-70571, 2020

[13] K. Y. Cheng, A. Y. Cho, T. J. Drummond, H. Morkoç, “Electron mobilities in modulation doped Ga0.47In0.53As/Al0.48In0.52 As heterojunctions grown by molecular beam epitaxy“, Appl. Phys. Lett. 15 January, 40 (2): 147–149, 1982

[14] Chin-An Chang, L. L. Chang, E. E. Mendez, M. S. Christie, L. Esaki “Electron densities in InAs–AlSb quantum wells”, J. Vac. Sci. Technol. B, 2 (2): 214–216, 1 April 1984

[15] H. L. Störmer, K. Baldwin, A. C. Gossard, and W. Wiegmann, "Modulation doped field effect transistor based on a two dimensional hole gas", Applied Physics Letters 44, 1062, 1984

[16] D. V. Lang, R. People, J. C. Bean, A. M. Sergent “Measurement of the band gap of GexSi1−x/Si strained-layer heterostructures”, Appl. Phys. Lett, 47 (12): 1333–1335, 15 December 1985

[17] A. Ketterson et al, "High transconductance InGaAs/AlGaAs pseudomorphic modulation-doped field-effect transistors", in IEEE Electron Device Letters, vol. 6, no. 12, pp. 628-630, Dec. 1985

[18] Abstreiter G, Brugger H, Wolf T, Jorke H, Herzog H, “Strain-induced two-dimensional electron gas in selectively doped Si/SixGe1-x superlattices. Phys Rev Lett, Jun 3;54(22):2441-2444., 1985

[19] H. Daembkes, H. . -J. Herzog, H. Jorke, H. Kibbel and E. Kasper, "The n-channel SiGe/Si modulation-doped field-effect transistor", IEEE Transactions on Electron Devices, vol. 33, no. 5, pp. 633-638, May 1986

[20] Fritz, Ian J. et al. “Influence of built-in strain on Hall effect in InGaAs/GaAs quantum well structures with p-type modulation doping”, Applied Physics Letters 49, pp 581-583 1986

[21] Razeghi, Manijeh et al, “First observation of two-dimensional hole gas in a Ga0.47In0.53As/InP heterojunction grown by metalorganic vapor deposition”, Journal of Applied Physics 60, 1986

[22] Pearsall, Thomas & Bean, J, “Enhancement and depletion-mode p-channel Ge(x)Si(1-x) modulation-doped FET's”, IEEE Electron Device Letters - IEEE ELECTRON DEV LETT. 7. 308-310, 1986

[23] P. C. Chao et al, "High performance 0.1 μm gate-length planar-doped HEMTs", 1987 International Electron Devices Meeting, Washington, DC, USA, pp. 410-413, 1987

[24] Lee, Chien-Ping et al, “High-transconductance p-channel InGaAs/AlGaAs modulation-doped field effect transistors”, IEEE Electron Device Letters 8, pp 85-87, 1987

[25] M. D. Feuer et al, "InP-based HIGFETs for complementary circuits", IEEE Transactions on Electron Devices, vol. 36, no. 11, pp. 2616-, Nov. 1989

[26] U. K. Mishra et al, "Impact of buffer layer design on the performance of AlInAs-GaInAs HEMTs," in IEEE Transactions on Electron Devices, vol. 36, no. 11, pp. 2616-, Nov. 1989

[27] L. F. Lester et al, "High-efficiency 0.25- mu m gate-length pseudomorphic power heterostructure FETs at millimeter-wave frequencies", IEEE Transactions on Electron Devices, vol. 36, no. 11, pp. 2616-2617, Nov. 1989

[28] W. Hansen, T. P. Smith, J. Piao, R. Beresford, W. I. Wang, “Magnetoresistance measurements of doping symmetry and strain effects in GaSb-AlSb quantum wells”, Appl. Phys. Lett. 1 January 1990

[29] L. F. Luo, K. F. Longenbach and W. I. Wang, "p-channel modulation-doped field-effect transistors based on AlSb/sub 0.9/As/sub 0.1//GaSb," in IEEE Electron Device Letters, vol. 11, no. 12, pp. 567-569, Dec. 1990

[30] M. Asif Khan, J. N. Kuznia, J. M. Van Hove, N. Pan, J. Carter, “Observation of a two-dimensional electron gas in low pressure metalorganic chemical vapor deposited GaN-AlxGa1−xN heterojunctions”, Appl. Phys. Lett. 15 June 1992; 60 (24): 3027–3029. https://doi.org/10.1063/1.106798

[31] M. Asif Khan, A. Bhattarai, J. N. Kuznia, D. T. Olson, “High electron mobility transistor based on a GaN-AlxGa1−xN heterojunction”, Appl. Phys. Lett. 30 August 1993; 63 (9): 1214–1215. https://doi.org/10.1063/1.109775

[32] Klem, J.F., Lott, J.A., Schirber, J.E. et al, “Strained quantum well modulation-doped ingasb/algasb structures grown by molecular beam epitaxy”, J. Electron. Mater. 22, 315–318 (1993)

[33] Pfeiffer, L. and West, K. W., “The role of MBE in recent quantum Hall effect physics discoveries”, Physica E Low-Dimensional Systems and Nanostructures, vol. 20, no. 1, pp. 57–64, 2003

[34] Umansky, Vladimir & Heiblum, M. & Levinson, Y. & Smet, J. & Nübler, J. & Dolev, Merav, “MBE growth of ultra-low disorder 2DEG with mobility exceeding 35 X 10^6 cm^2/Vs. Journal of Crystal Growth, pp 1658-1661, 2009

[35] Alamo, Del and Antonio Jesús. “The High-Electron Mobility Transistor at 30: Impressive Accomplishments and Exciting Prospects.”, 2011

[36] Dang, Phillip & Khalsa, Guru & Chang, Celesta & Katzer, D. & Nepal, Neeraj & Downey, Brian & Wheeler, Virginia & Suslov, Alexey & Xie, Andy & Beam, Edward & Yu, Cao & Lee, Cathy & Muller, David & Xing, Huili & Meyer, David & Jena, Debdeep, “An all-epitaxial nitride heterostructure with concurrent quantum Hall effect and superconductivity. Science Advances. 7, 2021

[37] Gassoumi, Moujahed, et al. “DC and RF Characteristics Optimization of Algan/Gan/Bgan/Gan/Si HEMT for Microwave-Power and High Temperature Application.” Results in Physics, Elsevier, 27 Nov. 2018

[38] SILVACO International, “ATLAS User’s Manual- Device Simulation Software”

[39] S. Chatterjee, A. Sengupta, S. Kundu and A. Islam, "Analysis of AlGaN/GaN high electron mobility transistor for high frequency application," 2017 Devices for Integrated Circuit (DevIC), Kalyani, India, 2017, pp. 196-199, doi: 10.1109/DEVIC.2017.8073935.

[40] Islam, Naeemul & Packeer, Fauzi & Khan, Muhammad & Falina, Shaili & Kawarada, Hiroshi & Syamsul, Ts. Dr. Mohd. (2022). Reliability, Applications and Challenges of GaN HEMT Technology for Modern Power Devices: A Review. Crystals. 12. 1581. 10.3390/cryst12111581.

[41] Das, J. & Oprins, Herman & Ji, Hangfeng & Sarua, A. & Ruythooren, W. & Derluyn, Joff & Kuball, Martin & Germain, Marianne & Borghs, Gustaaf. (2007). A Temperature Analysis of High-power AlGaN/GaN HEMTs.

[42] Dai, Pengfei & Wang, Shaowei & Lu, Hongliang. (2024). Research on the Reliability of Threshold Voltage Based on GaN High-Electron-Mobility Transistors. Micromachines. 15. 321. 10.3390/mi15030321.

[43] Aadit, Navid Anjum & Kirtania, Sharadindu & Afrin, Farhana & Alam, Md & Khosru, Q.D.M.. (2017). High Electron Mobility Transistors: Performance Analysis, Research Trend and Applications. 10.5772/67796.

[44] Chen, Kun-Ming & Lin, Chuang-Ju & Nagarajan, Venkatesan & Yi-Chang, Edward & Lin, Chao-Wen & Huang, Guo-Wei. (2021). Analysis of High-Frequency Behavior of AlGaN/GaN HEMTs and MIS-HEMTs under UV Illumination. ECS Journal of Solid State Science and Technology. 10. 10.1149/2162-8777/abf9eb.

[45] M. Gassoumi, A. Helali, H. Maaref, and M. Gassoumi, ‘DC and RF characteristics optimization of AlGaN/GaN/BGaN/GaN/Si HEMT for microwave-power and high temperature application’, Results in Physics, vol. 12, pp. 302–306, 2019.

[46] Y. Li et al., "Analysis of High-Frequency Behavior of AlGaN/GaN HEMTs and MIS-HEMTs under UV Illumination," Journal of the Electrochemical Society, vol. 171, no. 9, pp. 1-11, 2024, DOI: 10.1149/2162-8777/abf9eb.

[47] S., A., Jacob, B., Paul, G., & Suresh Babu, V. (2021). DC Characterization and High-Frequency Performance Analysis of a GaN/AlGaN HET on a β-Ga2O3 Substrate. IETE Journal of Research, 69(3), 1460–1465.

[48] Shashank Kumar Dubey, Meena Mishra, Aminul Islam, "Characterization of AlGaN/GaN based HEMT for low noise and high frequency application", Wiley Publication, 21 June 2021, DOI: 10.1002/jnm.2932.

[49] Krausse, Daniel & Quay, Rüdiger & Tessmann, Axel & Massler, Hermann & Leuther, A. & Merkle, Thomas & uller, S. & orer, C. & Mikulla, M. & Schlechtweg, Michael & Weimann, G.. (2004). Robust GaN HEMT low-noise amplifier MMICs for X-band applications.

[50] F. Lecourt et al., "High transconductance AlGaN/GaN HEMT with thin barrier on Si(111) substrate," 2010 Proceedings of the European Solid State Device Research Conference, Seville, Spain, 2010, pp. 281-284, doi: 10.1109/ESSDERC.2010.5618362.